



Field theory of survival probabilities, extreme values, first-passage times, and mean span of non-Markovian stochastic processes

Benjamin Walter ^{1,2,3,4,*} Gunnar Pruessner ^{1,2} and Guillaume Salbreux^{5,6}

¹Department of Mathematics, Imperial College London, 180 Queen's Gate, SW7 2AZ London, United Kingdom

²Centre for Complexity & Networks, Imperial College London, SW7 2AZ London, United Kingdom

³SISSA-International School for Advanced Studies, via Bonomea 265, 34136 Trieste, Italy

⁴INFN, Sezione di Trieste, 34136 Trieste, Italy

⁵The Francis Crick Institute, 1 Midland Road, NW1 1AT London, United Kingdom

⁶Department of Genetics and Evolution, University of Geneva, Quai Ernest-Ansermet 30, 1205 Geneva, Switzerland



(Received 23 December 2021; accepted 31 October 2022; published 19 December 2022)

We provide a perturbative framework to calculate extreme events of non-Markovian processes, by mapping the stochastic process to a two-species reaction-diffusion process in a Doi-Peliti field theory combined with the Martin-Siggia-Rose formalism. This field theory treats interactions and the effect of external, possibly self-correlated, noise in a perturbation about a Markovian process, thereby providing a systematic, diagrammatic approach to extreme events. We apply the formalism to Brownian motion and calculate its survival probability distribution subject to self-correlated noise.

DOI: [10.1103/PhysRevResearch.4.043197](https://doi.org/10.1103/PhysRevResearch.4.043197)

I. INTRODUCTION

Many nonequilibrium systems are studied by projecting out a single slow degree of freedom which evolves stochastically and often displays non-negligible memory effects [1–3]. A classic object of study is its survival probability, which describes the probability of the degree of freedom not having reached a threshold yet [4,5]. The survival probability defines not only the persistence exponents [6] but is also closely linked to the distribution of first-passage times, running maxima, and spans via some simple relations. All of these *extreme events* aptly characterize the nonequilibrium nature of complex systems and have been studied separately over the last hundred years (for classic references see Refs. [7–11]; for recent overviews, Refs. [12,13]).

Survival probabilities of non-Markovian processes are, however, notoriously hard to compute as they depend on the entire trajectory whose distribution is usually impossible to obtain [13–16]. Perturbative schemes such as those in Refs. [17,18] have proven to be successful in characterizing the behavior of the survival probabilities for large times in classical nonequilibrium models. More recently, a similar perturbation theory has been applied to fractional Brownian motion to further access the full survival probability in a perturbation theory about the Hurst parameter [15,19]. These techniques, however, heavily rely on Gaussianity and

do not readily translate to more general non-Gaussian non-Markovian processes.

In this article, we compute the *full* survival probability of processes subject to both uncorrelated and self-correlated noise in a perturbation theory in the strength of the self-correlated noise. A physical realization of such processes is a particle immersed in a heat bath and subject to a random self-propelling force. Our perturbative framework is valid in the regime where the self-correlated noise is small compared to thermal fluctuations stemming from the heat bath. More generally, this type of process is central to the study of active matter [20–24] and nonequilibrium phenomena [25–27].

In our recent work [28], we presented a scheme to calculate first-passage distributions for the same class of non-Markovian processes. These results relied on a perturbative functional expansion of a renewal-type equation inspired by the classical work of Refs. [10,29]. Using a field-theoretic approach that draws on both the Doi-Peliti [30,31] as well as the Martin-Siggia-Rose formalism [32], in the present work we generalize these results to a broader class of extreme events.

Using a field theory has some notable advantages. First, the diagrammatics give a clear intuition of the underlying microscopic processes otherwise hidden within cumbersome expressions. Second, the field theory provides a systematic perturbative framework naturally drawing on renormalization techniques. Third, it is easily extended to incorporate further interactions, such as reactions, and external and pair potentials.

This article is structured as follows. First, we map a Markovian process onto a field theory. Second, we introduce a field-theoretic mechanism which is designed to keep track of the space already visited by the process. This defines the visit probability $Q(x_0, x, t)$, the probability that the process started at x_0 has been at x prior to time t , and which is the complement

*bwalter@sissa.it

Published by the American Physical Society under the terms of the [Creative Commons Attribution 4.0 International](https://creativecommons.org/licenses/by/4.0/) license. Further distribution of this work must maintain attribution to the author(s) and the published article's title, journal citation, and DOI.

of the survival probability. Third, we add the self-correlated driving noise, thus breaking Markovianity, and compute the corrections induced in \mathcal{Q} . Finally, we illustrate the approach by computing the correction to the survival probability of Brownian motion driven by self-correlated noise.

II. FIELD THEORY FOR MARKOVIAN VISIT PROBABILITIES

A. Markovian transition probabilities

In this article, we construct a perturbation theory around Markovian processes characterized by a Langevin equation [33],

$$\begin{aligned} \dot{x}_t &= -V'(x_t) + \xi_t, \\ x(t = t_0) &= x_0, \end{aligned} \quad (1)$$

where $V'(x_t)$ is the gradient of a potential and ξ_t Gaussian white noise with correlator $\langle \xi_t \xi_{t'} \rangle = 2D_x \delta(t - t')$. Further, we introduce $T(x, t) \equiv T(x_0, x; t_0, t)$ as the *transition probability* for the walker to travel from x_0 at time t_0 to x at time t . This probability density is also known as the Green's function or propagator in related fields of mathematics. We will state x_0 and t_0 only where needed for clarity. The transition probability satisfies a Fokker-Planck equation [34],

$$\partial_t T(x, t) = (V''(x) + V'(x)\partial_x + D_x \partial_x^2) T(x, t), \quad (2)$$

with initial condition $T(x, t_0) = \delta(x - x_0)$.

As is detailed in Ref. [35], process (1) can be mapped to a Doi-Peliti field theory [35–37] containing two fields, the annihilator field $\varphi(x, t)$ and the creator field $\varphi^\dagger(x, t) = 1 + \tilde{\varphi}(x, t)$, which are jointly distributed according to

$$\mathcal{P}[\varphi, \tilde{\varphi}] = \exp(-\mathcal{S}_\varphi[\varphi, \tilde{\varphi}]). \quad (3)$$

Here the action $\mathcal{S}_\varphi[\varphi, \tilde{\varphi}]$ is constructed as

$$\mathcal{S}_\varphi = \iint dx dt \tilde{\varphi} (\partial_t - V''(x) - V'(x)\partial_x - D \partial_x^2) \varphi. \quad (4)$$

Moreover, the transition probability satisfies

$$T(x, t) = \langle \varphi(x, t) (1 + \tilde{\varphi}(x_0, t_0)) \rangle_{\mathcal{S}_\varphi}, \quad (5)$$

where $\langle \cdot \rangle_{\mathcal{S}_\varphi}$ denotes the expectation over the measure (3).

Constructing a solution to the partial differential equation in Eq. (2) via a path integral can in principle be done with the Feynman-Kac theorem [38,39]. Here, however, we use a nonequilibrium field theory following Ref. [32] (see Sec. V A 2 for further discussion).

B. Visit probability and extreme events

The key problem we address here is how to approximate the distribution of first-passage times, running maxima, and mean volume explored of the process defined in Eq. (1). These *extreme events* are all mutually related via the *visit probability* which we define as $\mathcal{Q}(x_0, x, t_0, t) = \mathcal{Q}(x, t) = \mathbb{P}[x_s = x \text{ at some time } t_0 \leq s \leq t]$, i.e., the complement of the *survival probability* $\mathbb{P}_{\text{surv}} = 1 - \mathcal{Q}$. This measures the probability that the particle has been at x at or before time t . In Fig. 1, we show a single realization of x_t , together with its visited area.

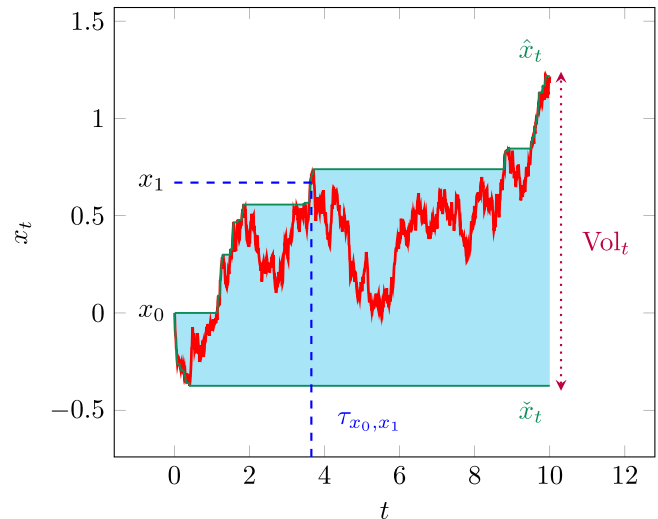


FIG. 1. A continuous random path x_t (red line) evolves in time. The *visited area* is shaded in blue. In this article, we study the visit probability $\mathcal{Q}(x, t)$, i.e., the probability that a point (x, t) lies within the blue area. As discussed in Sec. II B, the visit probability allows one to compute the distribution of (i) first-passage times τ_{x_0, x_1} [blue dashed line, Eq. (6)] and (ii) running maxima \hat{x}_t [green line, Eq. (7)], as well as (iii) the average volume explored [purple arrow, Eq. (8)].

The visit probability contains various information about the process: When taking the derivative $\partial_t \mathcal{Q}(x, t)$, one measures the weight of those paths which visit x at t for the first time. The latter is the first-passage time, shown in Fig. 1 as a blue dashed line, and thus its distribution satisfies

$$\mathbb{P}_{\text{FPT}}(\tau_{x_0, x_1} = t) = \partial_t \mathcal{Q}(x_1, t). \quad (6)$$

Analogously, taking the derivative $-\partial_x \mathcal{Q}(x, t)$ weighs those paths that at time t visit x for the first time or, alternatively, the distribution of the maximum $\hat{x}_t = \max_{s \leq t} x_s$, shown as a green line in Fig. 1, i.e.,

$$\mathbb{P}_{\text{Max}}(\hat{x}_t = x) = -\partial_x \mathcal{Q}(x, t), \quad (7)$$

for $x > x_0$. Moreover, integrating over $\int dx \mathcal{Q}(x, t)$ gives the average of the volume explored, which is defined as the difference between running maximum and minimum, $\text{Vol}([x_t], t) = \max_{s \leq t} x_s - \min_{s \leq t} x_s$, as illustrated in Fig. 1. Its mean is given by

$$\langle \text{Vol} \rangle = \int dx \mathcal{Q}(x, t). \quad (8)$$

Higher moments of the volume explored are considered in Ref. [40].

C. Overview of main results

In the following, we build a framework to compute the visit probability $\mathcal{Q}(x, t)$ for a specific class of non-Markovian processes. These are given by the solution to the stochastic differential equation

$$\dot{x}_t = -V'(x_t) + \xi_t + gy_t. \quad (9)$$

This equation extends the Markovian Langevin equation (1) by adding a second independent noise term y_t which is assumed to be stationary, of zero mean, but not necessarily Gaussian. The driving noise y_t further carries dimensions of

a velocity, leaving g as a dimensionless coupling constant which we suppose to be small. The main result of this article then is a perturbative expansion of the visit probability of x_t to leading order in g^2 ; i.e., assuming the visit probability allows for an analytical expansion around $g = 0$ as $Q(x, t) = Q^{(0)}(x, t) + g^2 Q^{(2)}(x, t) + \mathcal{O}(g^3)$, we find formulas for the correction terms. As is further detailed below, the assumption that $Q(x, t)$ is analytic in g restricts the possible choice of driving noises depending on the choice of potential $V(x_t)$. Together, Eqs. (28) and (29) provide a general formula for the leading perturbative correction, $Q^{(2)}(x, t)$, which is expressed in terms of the Markovian transition probability $T(x, t)$ and the two-time correlation function of y_t ,

$$C_2(t - s) = \overline{y_s y_t}, \tag{10}$$

where $\bar{\cdot}$ denotes the average with respect to the path measure of y_t .

In principle, the framework also allows to compute higher-order corrections, i.e., $g^n Q^{(n)}(x, t)$, using the n point correlations of the driving noise. In the presentation of the results, however, we restrict ourselves to the leading-order perturbation only.

The processes described by Eq. (9) do not satisfy a (generalized) fluctuation-dissipation relation, and hence cannot be brought into the form of a generalized Langevin equation. Instead, these processes are often used to model active matter in thermal environments [20–27], which typically operate away from equilibrium.

Finally, although the expression for the visit probability applies to all potentials $V(x)$, and can be employed numerically to study these, an analytically closed expression can only be expected in cases where an analytic solution to the Markovian Fokker-Planck equation (2) is known. This effectively reduces the class of potentials for which we obtain analytical results to harmonic or flat potentials, i.e., perturbations of Brownian motion or Ornstein-Uhlenbeck processes.

D. Markovian visit probabilities

In this section, we present a field theory of visit probabilities for Markovian processes. While in the case of transition probabilities it is well known that the solution to the Fokker-Planck equation (2) can be expressed as a path integral, Eq. (5), this has not yet been established for the visit probability $Q(x, t)$. Our aim is to construct a field theory whose correlation functions equal $Q(x, t)$, in close analogy to Eq. (5). In difference to the case for the transition probability, however, this field theory cannot be straightforwardly constructed for $Q(x, t)$, since no evolution equation for $Q(x, t)$, comparable to Eq. (2), exists to our knowledge.

As is explained in great detail in Refs. [40–42], and briefly discussed in Appendix A, the visit probability $Q(x, t)$ can be expressed as a field-theoretic expectation value under a Doi-Peliti field theory by introducing two additional auxiliary (“trace”) fields $\psi(x, t)$ and $\tilde{\psi}(x, t)$ with a joint distribution

$$\begin{aligned} &\mathcal{P}[\varphi, \tilde{\varphi}, \psi, \tilde{\psi}] \\ &= \lim_{\gamma \rightarrow \infty} \exp(-\mathcal{S}_\varphi[\varphi, \tilde{\varphi}] - \mathcal{S}_\psi[\psi, \tilde{\psi}] + \gamma \mathcal{S}_\gamma[\varphi, \tilde{\varphi}, \psi, \tilde{\psi}]) \end{aligned} \tag{11}$$

such that the visit probability can be written as

$$Q(x, t) = n_0^{-1} \langle \psi(x, t) (1 + \tilde{\varphi}(x_0, t_0)) \rangle_S, \tag{12}$$

where $\langle \cdot \rangle_S$ is understood as the average with respect to the measure in Eq. (11). Here, we have introduced a normalizing density n_0 which is further detailed below and in Appendix A.

The pair of fields $\psi, \tilde{\psi}$ is a stochastic auxiliary variable which tracks the volume explored by the process x_t (see Fig. 1). This is in analogy to $\varphi, \tilde{\varphi}$ whose correlation tracks the current position of the process x_t [cf. Eq. (5)]. Hence, measuring the average field density $\psi(x, t)$, and normalizing by a unit density n_0 , amounts to computing the probability that the process visited x up to time t . The average in Eq. (12) then corresponds to the probability density that x has been visited prior to t *conditioned* on the process having been initialized at x_0 at time t_0 , thus matching our definition of the visit probability.

The field action $\mathcal{S}_\varphi + \mathcal{S}_\psi - \gamma \mathcal{S}_\gamma$ consists of three actions which model (i) the diffusion of the process x_t [cf. Eq. (4)], (ii) the noninteracting dynamics of the auxiliary fields tracking the volume explored by the particle, and (iii) the interaction between the random process x_t and the auxiliary fields tracking its explored volume. Clearly, the explored volume depends on all the previous positions of the process x_t and therefore the third contribution contains all four fields $\varphi, \tilde{\varphi}, \psi, \tilde{\psi}$. It is multiplied with a rate γ to be taken to ∞ . This rate is interpreted as the rate with which the process x_t “traces,” i.e., marks as explored, a given point x . Taking $\gamma \rightarrow \infty$ amounts to the field ψ tracking *every* visited point.¹ In what follows, we outline the components of the action in Eq. (11) and refer the reader to the Appendixes for technical details.

The first term in the exponential of Eq. (11) is the *diffusion action* \mathcal{S}_φ introduced in Eq. (4). The second term \mathcal{S}_ψ denotes the *trace action*:

$$\mathcal{S}_\psi = \iint dx dt \tilde{\psi}(\partial_t + \varepsilon)\psi. \tag{13}$$

Comparing with \mathcal{S}_φ , Eq. (4), the trace action can be interpreted as corresponding to the process (1) with $V(x) \equiv 0$, $D_x = 0$, i.e., a deterministic immobile particle. This reflects the fact that a point, once visited by the process x_t , remains *visited* forever. To ensure convergence of the path integral over Eq. (11), we have included a positive parameter $\varepsilon > 0$. The latter further ensures causality [40,44], i.e., that a point is only marked visited *after* it has been visited by the process x_t . In a field-theoretic context, the parameter ε is referred to as a *mass* or an *infrared regulator* as it suppresses the divergencies otherwise arising in Eq. (11) from the contributions of Eq. (13) at large times. The parameter ε is to be taken to zero at the end of the calculation.

The third term of the exponential of Eq. (11) is the *deposition action*. It describes the growth of the volume explored due to fluctuations of the process x_t and is derived in Ref. [41].

¹Leaving γ finite amounts to imperfect tracking, suitable to study imperfect reaction kinetics as discussed in, e.g., Ref. [43].

In the continuum limit, it reads

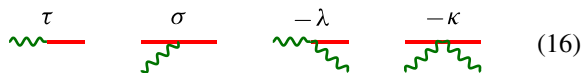
$$S_\gamma = \iint dx dt (\tau \tilde{\psi} \varphi + \sigma \tilde{\varphi} \tilde{\psi} \varphi - \lambda \tilde{\psi} \varphi \psi - \kappa \tilde{\varphi} \tilde{\psi} \varphi \psi). \tag{14}$$

The four dimensionfull couplings τ , σ , κ , and λ , are introduced differently for independent renormalization. However, the rates τ and σ and the densities κ and λ are each equal and are related to each other via

$$\lambda = \kappa = n_0^{-1} \tau = n_0^{-1} \sigma \tag{15}$$

(see Appendix A for details). Overall, S_γ is multiplied with a dimensionless constant γ which needs to be taken to $\gamma \rightarrow \infty$.

Each of the four vertices in Eq. (14) is diagrammatically represented as



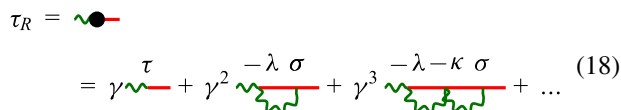
$$\begin{array}{cccc} \tau & \sigma & -\lambda & -\kappa \\ \text{---} & \text{---} & \text{---} & \text{---} \\ \text{wiggly} & \text{wiggly} & \text{wiggly} & \text{wiggly} \end{array} \tag{16}$$

and enters into the action multiplied by γ [see Eq. (11)]. Here, straight red lines represent the propagators of φ , $\tilde{\varphi}$, and green wiggly lines those of $\tilde{\psi}$, ψ . As a convention, we read vertices and diagrams from right to left.


It follows that the diagrammatic expansion of the trace function (12) is

$$Q(x, t) = n_0^{-1} \lim_{\gamma \rightarrow \infty} \begin{array}{c} (x, t) \\ \text{---} \\ \text{wiggly} \bullet \end{array} (x_0, t_0) \tag{17}$$

where the central dot stands for the renormalized coupling τ_R and the limit in $\gamma \rightarrow \infty$ stems from the definition of the action in Eq. (11). This renormalization is given by the diagrammatic expansion



$$\tau_R = \begin{array}{c} \text{---} \\ \text{wiggly} \bullet \end{array} + \gamma^2 \begin{array}{c} \text{---} \\ \text{wiggly} \bullet \end{array} + \gamma^3 \begin{array}{c} \text{---} \\ \text{wiggly} \bullet \end{array} + \dots \tag{18}$$

The only diagrams contributing to this expansion are chains of the loop diagram . We introduce the *return probability* $R(x, t) = T(x, x, t)$ and likewise its Fourier transform $R(x, \omega)$. As shown in Appendix B the fully renormalized vertex can be evaluated using a geometric sum as

$$\tau_R(\omega) = \frac{\gamma \tau}{1 + \gamma \kappa R(x, \omega)}, \tag{19}$$

which is an *exact* result for all γ , such that the effective trace function, Fourier transformed, is

$$\begin{aligned} \int dt e^{i\omega t} Q(x, t) &= n_0^{-1} \frac{1}{-i\omega + \varepsilon} \tau_R(\omega) T(x_0, x, \omega) \\ &= \frac{1}{-i\omega} \frac{T(x_0, x, \omega)}{R(x, \omega)}, \end{aligned} \tag{20}$$

where we made use of time-translational invariance to write the Fourier transform in one frequency only, tacitly took the limit $\varepsilon \rightarrow 0$, and used $\tau/\kappa = n_0$ [see Eq. (15)]. Multiplying this result with $(-i\omega)$ gives the first-passage-time moment-generating function. Then, the result in Eq. (20) agrees with classical results given in Refs. [10,29].

In summary, by introducing an extended field theory via the four-field action in Eq. (11), the visit probability of a Markovian process can be written as the field-theoretic average (12), in direct analogy to the (simpler) transition probability which can be represented with two fields [cf. Eq. (5)]. This effective field theory for visit probabilities comes at the cost of the additional fields ψ , $\tilde{\psi}$ which need to be related to the fields φ , $\tilde{\varphi}$ by a nonlinear interaction S_γ . The effect of this interaction on the growth of the volume explored by x_t can be captured by evaluating the effective (“renormalized”) deposition vertex τ_R . Formally, this amounts to evaluating an infinite series of correction terms, diagrammatically represented in Eq. (18). Using field-theoretic tools, the entire sum can be exactly evaluated [see Eq. (19)]. The result, Eq. (20), is in agreement with previous classical results. So far, we therefore have constructed a field theory for Markovian visit probabilities that reproduces known results. In the next section we consider non-Markovian processes, and use this field-theoretic formulation to compute the perturbative corrections to the exact result (20).

III. NON-MARKOVIAN VISIT PROBABILITIES: A PERTURBATIVE APPROACH

The process introduced in Eq. (1) is driven by δ -correlated noise and hence is Markovian [45]. As a perturbative generalization towards non-Markovian processes, we thus extend the class of processes given by Eq. (1) to

$$\dot{x}_t = -V'(x_t) + \xi_t + g y_t. \tag{21}$$

The additional driving noise y_t is assumed to be stationary with zero mean and a general autocorrelation function

$$C_2(t - s) = \overline{y_s y_t}. \tag{22}$$

By $\bar{\cdot}$ we denote in the following averages over the path distribution of y_t . Importantly, y_t is not required to be Gaussian such that higher nontrivial cumulants $C_n(t_2 - t_1, \dots, t_n - t_{n-1}) = \langle y_{t_1} \dots y_{t_n} \rangle_c$ may exist. Such higher-order cumulants enter only at perturbative order g^n . The correlation function $C_2(t - s)$ of the driving noise y_t may decay exponentially, such as for run-and-tumble particles in noisy environments [20,22], or algebraically.

In the following we perform a diagrammatic expansion of the visit probability $Q(x, t)$ in the dimensionless coupling constant g . Therefore, g is assumed to be small ($g \ll 1$). A condition for the validity of the expansion is that cumulants of the noise $C_n(t_2 - t_1, \dots, t_n - t_{n-1}) = \langle y_{t_1} \dots y_{t_n} \rangle_c$ are such that diagrams of the expansion are finite, for instance the diagram in Eq. (27). In what follows, we derive the visit probability $Q(x, t)$ averaged over both the Gaussian white noise ξ_t and the driving noise y_t to first leading perturbative order g^2 . For the case of Brownian motion driven by self-correlated noise, we find expressions that depend on a double integral of the cumulant $C_2(t)$, Eq. (31). Existence of this double integral allows for a broad class of correlation functions, even when $C_2(t)$ decays algebraically slowly at large times. Such algebraic decay occurs in processes driven by fractional Gaussian noise [21].

As is outlined in Appendix C, the visit probability conditioned on a *fixed realization* of the driving noise can still

$T(x_0, x, \omega) = T(x = x - x_0, \omega)$ of simple Brownian motion, $g = 0$, is given by $T(x, t) = (4\pi D_x t)^{-1/2} \exp(-\frac{x^2}{4D_x t})$, so that $T(x, \omega) = (\sqrt{-4i\omega D_x})^{-1} \exp(-\sqrt{-i\omega/D_x}|x|)$ and $\mathcal{Q}(x, t) = \mathcal{Q}^{(0)}(x, t) = 1 - \text{erf}((4D_x t)^{-1/2}|x|)$ via Eq. (20) and a subsequent inverse Fourier transform.

For $g \neq 0$, we compute the correction $T^{(2)}(x, \omega)$ using Eq. (29). As is detailed in Appendix F, the integral simplifies drastically, and we state here only the results, which can be summarized most succinctly using a “time-stretch function” $\Upsilon(t)$ as follows. Given the correlation function $C_2(t)$, Eq. (22), it is defined as

$$\Upsilon(t) = \int_0^t ds s C_2(t - s) = \int_0^t du \int_0^u ds C_2(s), \quad (31)$$

or, alternatively, $\partial_t^2 \Upsilon(t) = C_2(t)$ with $\Upsilon(0) = 0, \partial_t \Upsilon(t) = 0$. The second-order correction to the transition probability can then be written as

$$\begin{aligned} T^{(2)}(x_0, x, \omega) &= \int dt e^{i\omega t} \Upsilon(t) (\partial_{x_1}^2) T(x_0, x, t) \\ &= \int dt e^{i\omega t} D_x^{-1} \Upsilon(t) \partial_t T(x_0, x, t), \end{aligned} \quad (32)$$

$$\mathcal{Q}(x, \omega; g) = \mathcal{Q}^{(0)}(x, \omega) \left[1 + \frac{g^2}{D_x} \left(\frac{\int dt e^{i\omega t} \Upsilon(t) \partial_t T(x, t)}{T(x, \omega)} - \frac{\int dt e^{i\omega t} \Upsilon(t) \partial_t R(x, t)}{R(x, \omega)} \right) \right] + \mathcal{O}(g^3). \quad (34)$$

This relation illuminates the relation between the correction to the Fourier-transformed visit probability and the correlation function of the driving noise. To obtain the visit probabilities, and derive extreme event distributions, in real time [cf. Eqs. (6)–(8)], numerical integration will be necessary in most cases.

For exponentially correlated driving noise, such as “colored” or telegraphic noise, we have $C_2(t) = D_x \beta e^{-\beta|t|}$, Eq. (22), for some noise strength D_x and timescale of relaxation β^{-1} . The corresponding time-stretch function is

$$\Upsilon(t) = \frac{D_y}{\beta} (e^{-\beta t} + \beta t - 1). \quad (35)$$

From this function alone, one can read off that for large times the driving noise effectively shifts the diffusion constant by $D_x \rightarrow D_x + g^2 D_y$. At short timescales ($t \lesssim \beta^{-1}$), however, the correction is nontrivial.

We can further verify the validity of the expansion of the trace function $\mathcal{Q}(x, \omega; g)$, Eq. (34), by numerically inverting the Fourier transform and comparing to Monte Carlo simulations of the process in Eq. (30). To this end, we estimate numerically the probability that x_t has reached x_1 , at some given t and parameters such as g, D_x , and D_y , and subtract from it the exact result $\mathcal{Q}(x, t; g = 0)$. Plotting this difference over g^2 produces an estimate of the correction of $\mathcal{Q}(x, t; 0)$ to $\mathcal{Q}(x, t, g)$, described by Eq. (34) to leading order [see Eq. (G1) for explicit result]. Figure 3 shows this numerically estimated correction together with the inverted correction in Eq. (34).

where we made use of the Brownian relation $\partial_t T(x, t) = D_x \partial_x^2 T(x, t)$. In real time, the correction $T^{(2)}(x_0, x, t) = D_x^{-1} \Upsilon(t) \partial_t T(x, t)$ can be absorbed into the t dependence of the tree level as

$$T(x, t) = T(x, t + g^2 D_x^{-1} \Upsilon(t)) + \mathcal{O}(g^3). \quad (33)$$

This result is in agreement with the expression for the full transition probability found in Ref. [46], and is exact if y_t further is Gaussian. The externally driven non-Markovian process x_t has therefore transition probabilities that are, to order g^2 , equal to those of a time-stretched Brownian motion with $t \mapsto \tau(t) = (1 + g^2 (D_x t)^{-1} \Upsilon(t))t$, thus $x_t \stackrel{d}{=} \sqrt{2D_x} W_{\tau(t)}$. That, however, does not mean that the return probabilities agree between the original, externally driven non-Markovian process x_t and the time-stretched Brownian motion, because of the latter not accounting for the now hidden variable y_t (see also the discussion in Ref. [46]). The time-stretched Brownian motion ignores correlations between that y_t and x_t . For example, the transition probability is no longer correctly given by the first passage and repeated return, as first passage is favored for particular values of y_t that the subsequent return does not account for. Returning to Eq. (28), and using Eq. (32), we slightly rephrase the result for driven Brownian motion by explicitly expanding in g^2 to

The persistence exponent θ is defined as the tail exponent of the survival probability $\mathbb{P}_{\text{surv}}(x, t) = 1 - \mathcal{Q}(x, t) \sim t^{-\theta}$ [46]. It is also contained in the small ω expansion of the trace as $(-i\omega)^{-1} - \mathcal{Q}(x, \omega) \sim \omega^{\theta-1}$. Evaluating Eq. (34) using the time-stretch function (35) shows that the Markovian result of $\theta = \frac{1}{2}$ [4] does not acquire corrections as is expected for short-range correlated driving noise y_t .

V. DISCUSSION AND SUMMARY

In this section, we discuss our findings in the context of the literature of (quantum) field theory and stochastic dynamics and summarize our results.

A. Discussion

1. Relation to Markovian techniques

Our study is motivated by the study of complex systems comprising many interacting degrees of freedom of which we single out the slowest one as a stochastically evolving coordinate x_t (see Sec. I). The remaining degrees of freedom are subsumed into a bath, exerting a stochastic force onto the particle, here modeled by Eq. (21).

Often, the fast degrees of freedom in a complex system are assumed to evolve infinitely fast, thus rendering the stochastic evolution Markovian, since all correlations disappear within an infinitesimal time [47]. This assumption is reflected in the mathematical structure of the usual stochastic representations, such as Langevin equations [48,49] or Fokker-Planck equations [34] which evolve locally in time, i.e., with no

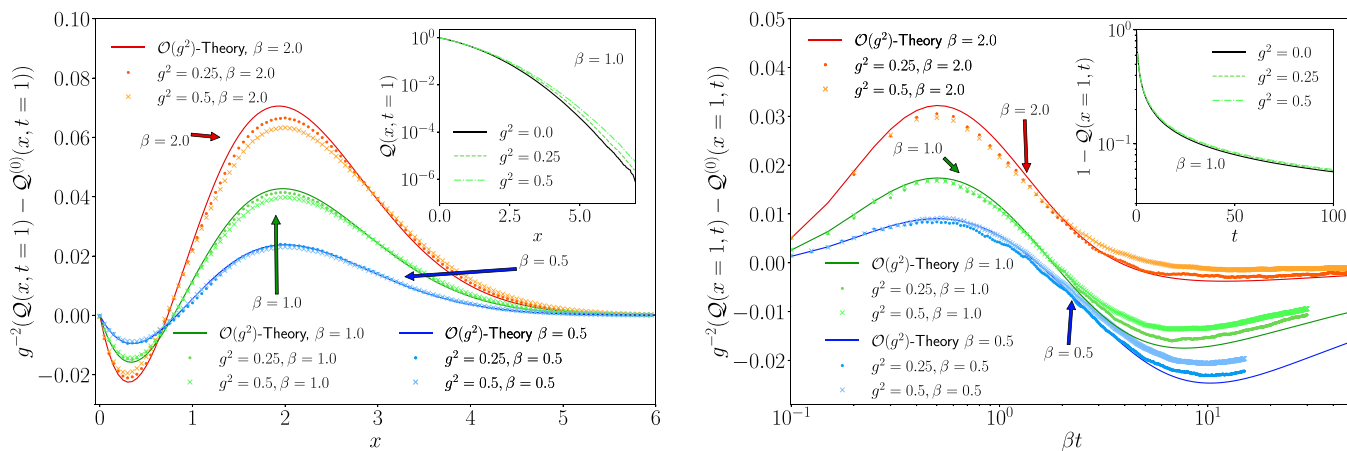


FIG. 3. Rescaled perturbative correction in g^2 to the visit probability $Q(x_1, t)$ of Brownian motion driven by correlated noise [ATBM; cf. Eq. (30)]. The left plot shows the result for fixed time, $Q(x_1, t = 1)$, and the right plot for fixed distance, $Q(x_1 = 1, t)$. The inset of the left plot shows the visit probability $Q(x_1, t = 1)$ over distance for simple Brownian motion ($g^2 = 0$, black line) as well as ATBM for $\beta = 1.0$ and $g^2 = 0.25$ (green dashed line), or $g^2 = 0.5$ (bright green dot-dashed line), respectively. The inset of the right plot shows the complement of the corresponding visit probability $1 - Q(x_1 = 1, t)$ over time, with identical parameters and symbols. The left (right) main panel shows the rescaled correction to the visit probability over distance x_1 (rescaled time βt) for three different values of, from top to bottom, $\beta = 2.0$ (red and orange), $\beta = 1.0$ (green), and $\beta = 0.5$ (blue). Plot marks indicate the result obtained from simulation for either $g^2 = 0.25$ (circles) or $g^2 = 0.5$ (crosses). The solid lines indicate our predictions to first leading order in g^2 obtained by calculating the result of Eq. (34) [cf. Eq. (G1)], and numerically inverting the Fourier transform. All simulations used $D_x = D_y = 1$, and $\geq 10^6$ realizations.

recourse to the past evolution. In this article, we set up a field-theoretic framework for Markovian processes in Sec. II. The “Markovianness” of the field theory can be seen from the field action (14) which is local in time. At this stage, the field theory is fully equivalent to any other Markovian description, and in fact reproduces the known Markovian result for the visit probability in Eq. (20).

The assumption of an infinitely fast evolving bath, however, is unphysical [47] and hence in each time increment the future stochastic evolution depends on the, potentially entire, past of the trajectory. This implies that the time-local formalisms mentioned above need to be extended to include nonlocal time interactions (e.g., to generalized Langevin equations [50] or fractional diffusion equations [51]). In our work, this self-interaction of the process with its own past is encapsulated by the nonlocal contribution (25). The self-interaction is most clearly seen diagrammatically by the loop diagram given in Eq. (27).

2. Field theory

Field-theoretically inspired path-integral methods are commonly used in the study of stochastic processes [52–56].

In this article, we begin by writing the solution of the Markovian ($g = 0$) forward equation (2), the transition probability $T(x, t)$, as a path integral in Eq. (5) over fields whose distribution is given by the action in Eq. (4). In setting up the field theory, Eq. (11), we constructed a nonequilibrium field theory using the Doi-Peliti formalism [30,31]. In principle, the transition probability can be obtained using alternative routes, following for instance the Feynman-Kac theorem [38,39] which expresses the solution to parabolic PDEs such as Eq. (2) as path integrals over trajectories rather than fields.

These alternative techniques, however, do not extend to either (i) the transition probability of driven, non-Markovian,

processes, such as Eq. (21), which render the forward equation nonlocal in time, or (ii) the stochastic description of the visit probability $Q(x, t)$ which to the best of our knowledge cannot be characterized as a solution to a parabolic PDE. This then requires two respective additional technical points with respect to alternative methods suitable to study transition probabilities of Markovian processes.

In order to address the average over the driving noise y_t , we introduced Eq. (26) where we replaced the path integral over the driving noise by its moment-generating function (or partition function) Z_y . Following field-theoretic standard procedures [57,58], we expand the latter in a power series in g . This is analogous to the perturbative treatment of self-interaction in classical field theories.

Second, in order to cast the visit probability $Q(x, t)$ (which does not readily follow from a Fokker-Planck equation) into a field theory, we used the tracing mechanism and its Doi-Peliti formulation to track the volume explored via the auxiliary fields $\psi, \tilde{\psi}$. This formalism (introduced in Ref. [41]) does not correspond to a classical field-theoretic technique, but is rooted in the study of reaction-diffusion methods with field-theoretic methods.

3. Stochastic dynamics

The problem of finding the transition probability, let alone the extreme event distribution, of non-Markovian processes has been a long-standing problem in stochastic dynamics. In terms of computing the transition probability, our field-theoretic approach recovers results known in the literature [46] in which non- δ -correlated driving noises are also treated using functional methods (see also Refs. [59,60] for a similar discussion of first-passage times). However, for non-Markovian processes the visit probability does not straightforwardly follow from the transition probability. The

visit probability $Q(x, t)$ therefore represents the central result of the present work.

B. Summary

In the present work we have established a method to compute the visit probability (the complement of the survival probability) for random motion in a one-dimensional potential, as defined in Eq. (21).

By mapping the problem to a field theory we systematically compute corrections to the Markovian result (20) to any order in the coupling g . The leading-order correction is of the form (28), which involves the g^2 -corrected transition probability given in Eq. (29). Generally, to compute the contribution to order g^n , it is sufficient to know the Markovian transition probability and the n -point function of the driving noise y_t . In the absence of an external potential, the expressions reduce to Eq. (34) which depends on the twice-integrated driving noise correlation $\Upsilon(t)$, Eq. (31).

By casting the problem in a field-theoretic language, we replaced the single degree of freedom by a field φ representing the full density. This allows us to extend the model to the case of many, potentially interacting, random walkers. Also, the Doi-Peliti framework allows for the inclusion of potentials. To the best of our knowledge, this is the first time that both Doi-Peliti and Martin-Siggia-Rose have been used simultaneously to construct an action.

Overall, we have established a method which further lays bare the interplay between non-Markovianness and extreme events in stochastic processes.

ACKNOWLEDGMENTS

B.W. and G.P. would like to thank the Francis Crick Institute for their hospitality. B.W. would like to thank Andrea Gambassi for insightful discussions and comments. B.W. acknowledges financial support from the MIUR-PRIN project ‘‘Coarse-grained description for non-equilibrium systems and transport phenomena (CO-NEST)’’ No. 201798CZL. G.S. was supported by the Francis Crick Institute which receives its core funding from Cancer Research UK (FC001317), the UK Medical Research Council (FC001317), and the Wellcome Trust (FC001317).

APPENDIX A: TRACING MECHANISM

The visit probability for Markovian processes [cf. Eq. (1)], given in Eq. (12), is a result that can be derived in various ways (indirectly, via the first-passage-time distribution, $\partial_t Q(x, t)$, this result has been found in, e.g., Ref. [10] using a renewal-type approach). Here, we derived the result by taking the continuum limit of a discrete reaction-diffusion process designed to track visits, which we refer to as a ‘‘tracing mechanism’’ and which has been introduced in Refs. [40,41].

To describe the tracing mechanism, we consider a coarse-grained version \mathfrak{r}_t of the stochastic process x_t of Eq. (1), which takes values only on a lattice $\delta_a \mathbb{Z}$ where δ_a is the lattice spacing, so that formally $\mathfrak{r}_t = \delta_a [\delta_a^{-1} x_t]$ where $[x]$ rounds to the nearest integer. At any time, the random walker attempts to deposit a *trace* at \mathfrak{r}_t with Poissonian rate proportional to γ . Each lattice site, however, has a ‘‘carrying capacity’’ \bar{n}_0

which limits the number of trace particles that can be deposited at this site. If at a site \bar{n}_0 trace particles have already been deposited, any further deposition is suppressed. Hence, the number of trace particles deposited at any lattice site is an integer bound above by \bar{n}_0 . Taking $\gamma \rightarrow \infty$, the particle deterministically deposits trace particles at any site visited for the first time. In the limit of $\delta_a \rightarrow 0$, the process \mathfrak{r}_t tends to x_t , and the expected number of trace particles at a site, divided by \bar{n}_0 , converges to $Q(x, t)$.

Cast into the language of reaction-diffusion processes, we have at each lattice site i

$$W_i + nT_i \xrightarrow{\gamma} W_i + (n+1)T_i, \quad n < \bar{n}_0, \quad (\text{A1})$$

$$T_i \xrightarrow{\varepsilon} \emptyset, \quad (\text{A2})$$

where particles of species W (‘‘walkers’’) deposit particles of species T (‘‘traces’’) at rate γ , provided their number does not surpass the carrying capacity \bar{n}_0 . Meanwhile W diffuses according to (a discretized form of) Eq. (1), and T remains at a given site and ‘‘evaporates’’ with rate ε , later sent to zero.

The Doi-Peliti formalism [30,31] describes the continuum limit of particle densities in a reaction-diffusion system, such as defined in Eqs. (A1) and (A2), by mapping the problem onto a nonequilibrium field theory, where each particle species corresponds to a pair of fields (see Ref. [41] for details). The local density of walkers, $\delta_a^{-1} W_i$, is mapped to $\varphi(x, t)$, $\tilde{\varphi}(x, t)$ (referred to as annihilation and creation fields, respectively), and the trace particle density $\lim_{\delta_a \rightarrow 0} \delta_a^{-1} T_i$ to $\psi(x, t)$, $\tilde{\psi}(x, t)$. As shown in Refs. [40,41], the joint distribution of the four fields then follows from the Doi Peliti framework to be distributed according to the action given in Eqs. (4), (11), and (14). In order to turn the density of tracers into a probability of visit, it needs to be divided by the normalizing density n_0 corresponding to the continuum limit of \bar{n}_0 . Hence, the field-theoretic formula for the visit probability, Eq. (12), contains a prefactor of n_0^{-1} .

APPENDIX B: FIELD-THEORETIC CALCULATION OF MARKOVIAN VISIT PROBABILITY

We derive Eq. (20), the expression for the visit probability in the Markovian case. First, we consider the field theory in the case of $\gamma = 0$, when the probability measure (11) is Gaussian.

We introduce the forward and backward operators $\mathcal{L}, \mathcal{L}^\dagger$,

$$\mathcal{L}(x) = V''(x) + V'(x)\partial_x + D_x \partial_x^2, \quad (\text{B1})$$

$$\mathcal{L}^\dagger(x) = -V'(x)\partial_x + D_x \partial_x^2, \quad (\text{B2})$$

associated to Eq. (1) and generating the corresponding Fokker-Planck equation

$$\begin{aligned} \partial_t T(x, t) &= \mathcal{L}T(x, t), \\ T(x, t = t_0) &= \delta(x - x_0), \end{aligned} \quad (\text{B3})$$

with $T(x, t)$ the transition probability of the process. The forward and backward operators have a set of eigenfunctions

$$\mathcal{L}u_n(x) = -\lambda_n u_n(x), \quad (\text{B4})$$

$$\mathcal{L}^\dagger v_n(x) = -\lambda_n v_n(x), \quad (\text{B5})$$

with eigenvalues $0 \leq \lambda_0 < \lambda_1 < \dots$. The eigenfunctions are L^2 normalized to satisfy the orthonormal relation

$$\int dx u_m(x)v_n(x) = \delta_{mn}, \tag{B6}$$

and since they form a complete set in L^2 they further satisfy [34]

$$\sum_n v_n(x_1)u_n(x_2) = \delta(x_1 - x_2). \tag{B7}$$

Thus, every field $\varphi, \tilde{\varphi}, \psi, \tilde{\psi}$ has a unique decomposition into the $u_n(x), v_n(x)$ in space. Together with a Fourier transform in time, we then write

$$\varphi(x, t) = \int d\omega \sum_k \varphi_k(\omega)u_k(x)e^{-i\omega t}, \tag{B8}$$

$$\tilde{\varphi}(x, t) = \int d\omega \sum_k \tilde{\varphi}_k(\omega)v_k(x)e^{-i\omega t}, \tag{B9}$$

and analogously for $\psi, \tilde{\psi}$ with coefficients $\psi_k(\omega), \tilde{\psi}_k(\omega')$, respectively. This *mode transform* diagonalizes the nonperturbative parts of the action, \mathcal{S}_φ and \mathcal{S}_ψ [cf. Eq. (11)], which read

$$\mathcal{S}_\varphi[\varphi, \tilde{\varphi}] = \int d\omega \sum_n \tilde{\varphi}_n(-\omega)(-i\omega + \lambda_n)\varphi_n(\omega), \tag{B10}$$

$$\mathcal{S}_\psi[\psi, \tilde{\psi}] = \int d\omega \sum_n \tilde{\psi}_n(-\omega)(-i\omega + \varepsilon)\psi_n(\omega). \tag{B11}$$

For $\gamma = 0$, the measure in Eq. (11) is Gaussian and the (Fourier-transformed) bare propagators of both fields, $\langle \varphi \tilde{\varphi} \rangle$ and $\langle \psi \tilde{\psi} \rangle$, therefore immediately follow from Eqs. (B10) and (B11) using standard path-integral techniques [61],

$$\langle \varphi_n(\omega') \tilde{\varphi}_m(\omega) \rangle = \frac{\delta_{m,n} \delta(\omega + \omega')}{-i\omega' + \lambda_n} = \text{---} \tag{B12}$$

$$\langle \psi_n(\omega') \tilde{\psi}_m(\omega) \rangle = \frac{\delta_{m,n} \delta(\omega + \omega')}{-i\omega' + \varepsilon} = \text{~~~~~} \tag{B13}$$

where we introduced a diagrammatic representation for both bare propagators. These propagators are commonly interpreted as the (linear) response functions [61]. Using Eq. (5), and transforming back into real space and time using Eqs. (B8) and (B9), we obtain the transition probability

$$T(x, t) = \sum_n v_n(x_0)u_n(x)e^{-\lambda_n(t-t_0)}\Theta(t - t_0), \tag{B14}$$

where $\Theta(t)$ is the Heaviside Θ function. Crucially, we made use of the property [44,61]

$$\langle \varphi \rangle_S = 0 \tag{B15}$$

such that $\langle \varphi(1 + \tilde{\varphi}) \rangle = \langle \varphi \tilde{\varphi} \rangle$.

We next consider the expectation (5) in the case of $\gamma \neq 0$ when the nonlinear contributions of \mathcal{S}_γ , Eq. (14), enter. Each of the four vertices is diagrammatically represented as

$$\begin{matrix} \tau & \sigma & -\lambda & -\kappa \\ \text{---} & \text{---} & \text{~~~~~} & \text{~~~~~} \end{matrix} \tag{B16}$$

and enters into the action multiplied by γ . Following Refs. [40,41], we introduce the *carrying-capacity density* n_0 which is the continuum limit of $\delta_a^{-1} \bar{n}_0$, where \bar{n}_0 is the maximal number of trace particles which can simultaneously be deposited at a single site. At bare level, the carrying capacity enters in the couplings via the relation

$$\lambda = \kappa = n_0^{-1} \tau = n_0^{-1} \sigma. \tag{B17}$$

It follows that the diagrammatic expansion of the trace function (12), which counts the average number of tracer particles at a site, needs to be normalized with n_0^{-1} in order to indicate the *visit probability*, and hence


$$\mathcal{Q}(x, t) = n_0^{-1} \lim_{\gamma \rightarrow \infty} \text{---} \tag{B18}$$

$$\begin{aligned} & \int dt e^{i\omega t} \mathcal{Q}(x, t) \\ &= n_0^{-1} \langle \psi(x) \tilde{\psi}(x) \rangle \left(\lim_{\gamma \rightarrow \infty} \tau_R(\omega) \right) \langle \varphi(x, \omega) \tilde{\varphi}(x_0, \omega) \rangle \end{aligned} \tag{B19}$$

$$= n_0^{-1} \frac{1}{-i\omega + \varepsilon} \left(\lim_{\gamma \rightarrow \infty} \tau_R(\omega) \right) T(x_0, x, \omega), \tag{B20}$$

where the central dot in the diagram stands for the renormalized coupling τ_R , and $T(x_0, x, \omega)$ is the Fourier transform of the transition probability. This renormalization of τ is given by the diagrammatic expansion of the amputated vertex

$$\tau_R = \text{---} = \gamma \text{---} + \gamma^2 \text{---} + \gamma^3 \text{---} + \dots \tag{B21}$$

The only diagrams contributing to this expansion are chains of the loop diagram , referred to in the following as a ‘‘bubble.’’ Considering the expansion in Fourier and mode transform, Eqs. (B8) and (B9) (see Appendix D for details), each diagram factorizes into a product over the bubbles and can hence be evaluated using a geometric or Dyson sum (see Appendix D for derivation), resulting in

$$\tau_R(\omega_1) = \frac{\gamma \tau}{1 + \gamma \kappa R(x_1, \omega_1)} \tag{B22}$$

such that the effective trace function, Fourier transformed, is

$$\begin{aligned} & \int dt e^{i\omega t} \mathcal{Q}(x, t) \\ &= \lim_{\gamma \rightarrow \infty} \frac{1}{-i\omega + \varepsilon} \frac{\gamma \tau n_0^{-1}}{1 + \gamma \kappa R(x_1, \omega + i\varepsilon)} T(x_0, x, \omega) \\ &= \frac{1}{-i\omega + \varepsilon} \frac{T(x_0, x, \omega)}{R(x_1, \omega + i\varepsilon)}, \end{aligned} \tag{B23}$$

where we made use of time-translational invariance to write the Fourier transform in one frequency only. The couplings τ/κ in Eq. (B22) cancel with n_0^{-1} following their bare values, Eq. (B17). This then leads to the central Markovian result for the trace function

$$\mathcal{Q}(x, t) = \int d\omega e^{-i\omega t} \frac{T(x_0, x, \omega)}{(-i\omega)R(x, \omega)}, \tag{B24}$$

where we have tacitly taken the limit $\varepsilon \rightarrow 0$.

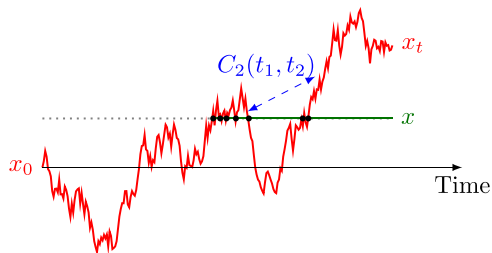


FIG. 4. The random walker x_t (red solid path) travels from $x_0 < x_1$ to $x_t > x_1$, thereby passing x_1 (green solid line) infinitely often (black dots). If the random walker is additionally driven by self-correlated noise [cf. Eq. (21)], this induces correlations between increments at any different times t_1, t_2 (blue dashed line). Meanwhile the perturbative expansion in γ [cf. Eq. (18)] tracks the probability of all possible transitions $T(x_1, t)$ and subsequent returns from x_0 to x_1 ; the second perturbative expansion in g includes the effect of correlated increments. If $g = 0$, the Markovian case, the process undergoes renewal at every return at x_1 , thus rendering the results such as Eq. (B23) exact.

APPENDIX C: VISIT PROBABILITY FOR DRIVEN PROCESS

In this Appendix, we provide some technical details to the derivation of the key result of Eqs. (28) and (29) which together provide the visit probability for non-Markovian processes of the form (21).

There are three technical steps: First, we consider the perturbative correction of the visit probability in the presence of a fixed, but random, realization of the driving noise y_t . Second, we average over all such realizations of y_t . This then leads to a large set of correction terms which we interpret diagrammatically and which, third, we evaluate to leading perturbative order.

1. Averaging general observables over driving noise

The presence of the autocorrelated driving noise y_t affects the transition and return probabilities of the random walker x_t (see Fig. 4). Conditioned on a fixed realization of y_t , the forward operator [cf. Eqs. (1), (B3), (B1), and (21)] is shifted by

$$\mathcal{L} \mapsto \mathcal{L} + g y_t \partial_x \varphi(x, t). \quad (\text{C1})$$

Hence, the y_t -conditioned random walker action in Eq. (4), which is essentially of the form $\tilde{\varphi}(\partial_t - \mathcal{L})\varphi$, is shifted also:

$$\mathcal{S}_\varphi[y_t] = \iint dx dt \tilde{\varphi}(\partial_t - \mathcal{L} - g y_t \partial_x)\varphi. \quad (\text{C2})$$

To obtain the y -averaged joint distribution of the four fields, one needs to evaluate [Eqs. (11), (23)]

$$\begin{aligned} & \overline{\mathcal{P}[\varphi, \tilde{\varphi}, \psi, \tilde{\psi}]} \\ &= \lim_{\gamma \rightarrow \infty} \int \mathcal{D}[y_t] \exp(-\mathcal{S}_\varphi[\varphi, \tilde{\varphi}] - \mathcal{S}_\psi[\psi, \tilde{\psi}]) \\ &+ \gamma \mathcal{S}_\gamma[\varphi, \tilde{\varphi}, \psi, \tilde{\psi}] + \iint g y_t \tilde{\varphi} \partial_x \varphi \mathcal{P}[y_t], \end{aligned} \quad (\text{C3})$$

where $g y_t \tilde{\varphi} \partial_x \varphi$ may be interpreted as a new vertex [see Eq. (27)]. While we were able to compute the result exactly in γ , we need to resort to perturbative methods to approximate in small couplings g . Although the path integral in Eq. (23) appears to require complete knowledge of the full path measure $\mathcal{P}[y_t]$ of the driving noise y_t , we can relax this requirement by introducing the normalized partition function (or moment-generating function) of y_t ,

$$\mathcal{Z}_y[g \cdot j_t] = \int \mathcal{D}[y_t] \exp\left(g \int dt j_t y_t\right) \mathcal{P}[y_t] \quad (\text{C4})$$

$$= 1 + \frac{1}{2} g^2 \iint dt_1 dt_2 j_{t_1} C_2(t_2 - t_1) j_{t_2} + \mathcal{O}(g^3), \quad (\text{C5})$$

where we ignore terms of higher perturbative order. We may thus replace the y_t integration in Eq. (23) by inserting $\mathcal{Z}_y[g \iint dx dt \tilde{\varphi} \partial_x \varphi]$ into expectations over the fields and consequently evaluate double averages via

$$\overline{\langle \bullet \rangle}_{\mathcal{S} + g y} = \left\langle \bullet \cdot \mathcal{Z}_y \left[g \iint dx dt \tilde{\varphi} \partial_x \varphi \right] \right\rangle_{\mathcal{S}}. \quad (\text{C6})$$

For example, the transition probability, averaged over all driving noises y_t , acquires a correction term which up to g^2 reads

$$\begin{aligned} T(x, t) &= \langle \varphi(x, t) \tilde{\varphi}(x_0, 0) \rangle + g^2 \iint dy_1 ds_1 dy_2 ds_2 \\ &\times C_2(s_2 - s_1) \langle \varphi(x, t) \tilde{\varphi}(y_1, s_1) \partial_{y_1} \varphi(y_1, s_1) \\ &\times \tilde{\varphi}(y_2, s_2) \partial_{y_2} \varphi(y_2, s_2) \tilde{\varphi}(x_0, 0) \rangle_{\mathcal{S}} + \mathcal{O}(g^4). \end{aligned} \quad (\text{C7})$$

The remaining field average in Eq. (C7) can now be evaluated normally, using standard Wick product rules (see Appendix B), Eq. (5), and the nondriven path measure (11). A straightforward calculation shows that the only nonvanishing correction to order g^2 in Eq. (C7) is

$$\begin{aligned} & g^2 \int_0^t ds_1 \int_0^{s_1} ds_2 \iint dy_1 dy_2 T(y_1, x, t - s_1) \\ & \times (\partial_{y_1} T(y_2, y_1, s_1 - s_2)) C_2(s_1 - s_2) (\partial_{y_2} T(x, y_2, s_1)), \end{aligned} \quad (\text{C8})$$

using $\langle \varphi(x_1, t) \tilde{\varphi}(y_1, s_1) \rangle = T(y_1, x_1, t - s_1)$, $\langle \partial_{y_1} \varphi(y_1, t) \tilde{\varphi}(y_2, s_1) \rangle = \partial_{y_1} T(y_2, y_1, s_1 - s_2)$, etc. Here, and in particular for more cumbersome expressions, it is advantageous to use diagrammatics to keep track of perturbative correction terms. The correction of the transition probability in Eq. (C8) is represented as

$$g^2 \quad x, t \quad \text{---} \quad \text{---} \quad \text{---} \quad x_0 \quad (\text{C9})$$

$\begin{array}{c} \text{---} \text{---} \text{---} \\ | \quad | \\ y_1, s_1 \quad y_2, s_2 \end{array}$

As in Eq. (B12), red solid lines denote bare transition probabilities. The blue dashed line connecting two internal vertices, Eq. (23), represents the correlation kernel $C_2(s_2, s_1)$. The two vertical bars inserted to the right of each such vertex represent the gradient operator acting on the target point of the incoming transition probability. As usual for Feynman diagrams, external fields depend on fixed parameters (x_0, x, t) , while

internal fields depend on variables to be integrated over (e.g., y_1, s_1, y_2, s_2). In addition to providing a better overview of terms arising in the perturbative expansion, diagrams also act as graphical cues illustrating how the driving noise induces memory into the evolution of x_t .

2. The driving noise averaged visit probability

Following Eq. (26), we are able to evaluate driving noise averaged observables. In order to derive the central results of Eqs. (28) and (29), it remains to evaluate the driving noise averaged visit probability

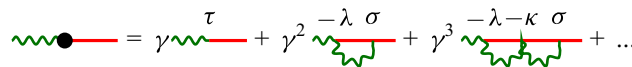
$$\mathcal{Q}(x, t) = \left\langle \psi(x, t) \tilde{\varphi}(0, 0) \mathcal{Z}_y [g \int \tilde{\varphi} \nabla \varphi] \right\rangle_S \tag{C10}$$

$$= \left\langle \psi(x, t) \varphi(x_0, 0) \left(1 + g^2 \iint dy_{1,2} ds_{1,2} \tilde{\varphi}_1 \partial_{y_1} \varphi_1 C_2(s_1 - s_2) \tilde{\varphi}_2 \partial_{y_2} \varphi_2 \right) \right\rangle_S + \mathcal{O}(g^3), \tag{C11}$$

where we use $\varphi_i = \varphi(y_i, s_i)$ for brevity. Each term appearing in the γ -perturbative expansion of the trace function [cf. Eq. (18)] is additionally corrected to order g^2 by replacing two internal $\tilde{\varphi}$ propagators by two “ y_t -driven propagators” $\tilde{\varphi} \partial_x \varphi$ and connecting them with the two-point correlator C_2 of y_t . As can be seen easiest diagrammatically, all possible corrections fall into one of the four categories shown in Fig. 2. They are classified according to whether both g vertices couple to the same or different propagator of a transition or a return. It is simplest to compute the four contributions in frequency rather than direct time as the loops factorize. The calculation itself is given in Appendix E.

APPENDIX D: RENORMALIZATION OF TRANSMUTATION RATE

In this Appendix, we derive the result for the renormalization of the coupling τ which is stated in Eq. (19). To simplify the computation, we perform the calculation in x, ω variables, i.e., in real space and Fourier transformed time. The renormalization is given by [cf. Eq. (18)]



$$\text{Diagram} = \tau + \gamma^2 \text{Diagram} + \gamma^3 \text{Diagram} + \dots \tag{D1}$$

which is a diagrammatic representation of the terms arising in the path-integrated average of the visit probability, Eq. (12), when expanding in γ ,

$$\begin{aligned} n_0^{-1} \langle \psi(x, \omega_1) \tilde{\varphi}(x_0, \omega_0) \rangle_S &= n_0^{-1} \gamma \tau \iint dz d\omega' \langle \psi(x, \omega_1) \tilde{\psi}(z, \omega') \varphi(z, \omega') \tilde{\varphi}(x_0, \omega_0) \rangle_{S; \gamma=0} \\ &\quad - n_0^{-1} \gamma^2 \lambda \sigma \iint dz_1 dz_2 d\omega'_1 d\omega'_2 d\omega''_1 d\omega''_2 \langle \psi(x, \omega_1) \tilde{\psi}(z_1, -\omega'_1 - \omega''_1) \psi(z_1, \omega_1'') \rangle \\ &\quad \times \varphi(z_1, \omega'_1) \tilde{\psi}(z_2, \omega_2'') \tilde{\varphi}(z_2, \omega'_2) \varphi(z_2, -\omega'_2 - \omega''_2) \tilde{\varphi}(x_0, \omega_0) \rangle_{S; \gamma=0} + \dots \end{aligned} \tag{D2}$$

Crucially, the averages $\langle \cdot \rangle_{S; \gamma=0}$ are taken over Gaussian random variables since for $\gamma = 0$ the path action [Eq. (11)] is bilinear. Thus, Wick’s theorem (e.g., Ref. [57]) applies and all averages in Eq. (D2) decompose into products of two-point functions. The only such Gaussian two-point functions which do not vanish are

$$\langle \varphi(z_1, \omega_1) \tilde{\varphi}(z_0, \omega_0) \rangle_{S; \gamma=0} = T(z_0, z_1; \omega_1) \delta(\omega_0 + \omega_1) = \int dt e^{i\omega_1(t-t_0)} T(z_0, z_1; t) \delta(\omega_0 + \omega_1), \tag{D3}$$

$$\langle \psi(z_1, \omega_1) \tilde{\psi}(z_0, \omega_0) \rangle_{S; \gamma=0} = \frac{\delta(z_1 - z_0) \delta(\omega_0 + \omega_1)}{-i\omega_1 + \varepsilon} = \iint dt_0 dt e^{i\omega_1 t + i\omega_0 t_0} \Theta(t - t_0) \delta(z_1 - z_0) e^{-\varepsilon(t-t_0)}. \tag{D4}$$

The second correlator intuitively characterizes the behavior of the trace which, once deposited at z_0 at time t_0 , remains there for an infinitely long time, as $\varepsilon \rightarrow 0$. Equipped with these correlators, the nonvanishing contributions to the averages appearing in Eq. (D2) are, following Wick’s theorem,

$$\begin{aligned} n_0^{-1} \gamma \tau \iint dz d\omega' \langle \psi(x, \omega_1) \tilde{\psi}(z, \omega') \varphi(z, \omega') \tilde{\varphi}(x_0, \omega_0) \rangle_{S; \gamma=0} &= n_0^{-1} \gamma \tau \iint dz d\omega' \frac{\delta(x - z) \delta(\omega_1 + \omega')}{-i\omega_1 + \varepsilon} T(x_0, z, \omega') \delta(\omega' + \omega_0) \\ &= n_0^{-1} \gamma \tau \frac{T(x_0, x, -\omega_1)}{-i\omega_1 + \varepsilon} \delta(\omega_0 - \omega_1), \end{aligned} \tag{D5}$$

and to second order,

$$-n_0^{-1} \gamma^2 \lambda \sigma \iint dz_1 dz_2 d\omega'_1 d\omega'_2 d\omega''_1 d\omega''_2 \tag{D6}$$

$$\times \langle \psi(x, \omega_1) \tilde{\psi}(z_1, -\omega'_1 - \omega''_1) \psi(z_1, \omega_1'') \varphi(z_1, \omega'_1) \tilde{\psi}(z_2, \omega_2'') \tilde{\varphi}(z_2, \omega'_2) \varphi(z_2, -\omega'_2 - \omega''_2) \tilde{\varphi}(x_0, \omega_0) \rangle_{S; \gamma=0}$$

$$= -n_0^{-1} \gamma^2 \lambda \sigma \frac{1}{-i\omega_1 + \varepsilon} \int d\omega''_2 \frac{R(x, x, \omega_1 - \omega''_2)}{-i\omega''_1 + \varepsilon} T(x_0, x, \omega_0) \delta(\omega_0 + \omega_1) \tag{D7}$$


$$= -n_0^{-1} \gamma^2 \lambda \sigma R(x, \omega_1 + i\varepsilon) \frac{T(x_0, x, \omega_0)}{-i\omega_1 + \varepsilon} \delta(\omega_0 + \omega_1), \tag{D8}$$

where in the first equality we used the definition of the return probability to abbreviate

$$\iint dz_1 dz_2 \delta(x - z_1) \delta(z_1 - z_2) T(z_1, z_2, \omega) = R(x, \omega), \tag{D9}$$

and in the second equality used Cauchy's residue formula to solve the integral by evaluating the residue of the simple pole at $\omega''_2 = -i\varepsilon$.

Since both correlators in Eq. (D3) are proportional to $\delta(\omega_0 + \omega_1)$, all higher-order expansion terms factorize, after integrating over the internal frequencies, into a product over amputated one-loop bubble diagrams (i.e., interpreted here as a function of external parameters z_1, ω_1 and z_2, ω_2 , respectively) which by analogous reasoning to the calculation above evaluate as

$$z_1, \omega_1 \text{  } z_2, \omega_2 = \gamma^2 \lambda \sigma R(z_1, \omega_1 + i\varepsilon) \delta(\omega_1 + \omega_2) \delta(z_1 - z_2). \tag{D10}$$

The bubble diagram graphically encodes the probability of a particle depositing a trace and then returning to it, in other words a "time-ordered" return probability: The green wiggly line may be understood as the trace which once placed remains immobile; meanwhile the red solid line represents the diffusing, and returning, walker. Likewise, the higher-order diagrams in Eq. (18) may be interpreted as repeated returns to x .

Returning to Eq. (18), the renormalized τ coupling, τ_R , is the effective factor satisfying

$$\langle \psi(x, \omega_1) \tilde{\varphi}(x_0, \omega_0) \rangle_S = \frac{1}{-i\omega_1 + \varepsilon} \tau_R(\omega_1) T(x_0, x, -\omega_0) \delta(\omega_0 + \omega_1) \tag{D11}$$

and, collecting the factors generated by the terms in Eq. (D2) and evaluated using Eq. (D10), one obtains

$$\tau_R(\omega_1) = \gamma \text{  } + \gamma^2 \text{  } + \gamma^3 \text{  } + \dots \tag{D12}$$

$$= [\gamma \tau - \gamma^2 \lambda \sigma R(x, \omega_1 + i\varepsilon) + \gamma^3 \lambda \sigma \kappa (R(x, \omega_1 + i\varepsilon))^2 - \gamma^4 c \sigma \kappa^2 (R(x, \omega_1 + i\varepsilon))^3 + \dots] \delta(\omega_0 + \omega_1). \tag{D13}$$

This series can be resummed using the geometric series, in field theory often referred to as Dyson summation [57]. Rearranging the sum gives

$$\tau_R(\omega_1) = \left[\gamma \tau + \gamma \frac{\lambda \sigma}{\kappa} \sum_{r=1}^{\infty} (-\gamma \kappa R(x, \omega_1 + i\varepsilon))^r \right] \tag{D14}$$

$$= \left[\gamma \tau + \gamma \frac{\lambda \sigma}{\kappa} \sum_{r=0}^{\infty} (-\gamma \kappa R(x, \omega_1 + i\varepsilon))^r - \gamma \frac{c \sigma}{\kappa} \right] \tag{D15}$$

$$= \left[\frac{\gamma \tau}{1 + \gamma \kappa R(x, \omega_1 + i\varepsilon)} + \gamma \left(\underbrace{\tau - \frac{c \sigma}{\kappa}}_{=0} \right) \right] \tag{D16}$$

$$= \frac{\gamma \tau}{1 + \gamma \kappa R(x, \omega_1 + i\varepsilon)}, \tag{D17}$$

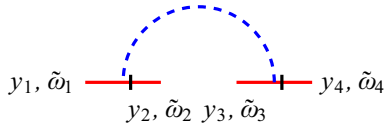
where we made use of the bare values given in Eq. (14); i.e., we replaced σ with τ and used $\lambda = \kappa$ at bare level. This vertex interpolates the physical pictures for $\gamma = 0$, where no deposition takes place ($\tau_R = 0$), and $\gamma \rightarrow \infty$, where every newly visited site gets marked immediately by a deposited trace. For $\gamma \rightarrow \infty$, the coupling tends to

$$\lim_{\gamma \rightarrow \infty} \tau_R(\omega_1) = \frac{n_0}{R(x, \omega_1 + i\varepsilon)}, \tag{D18}$$

using $n_0 = \tau/\kappa$.

APPENDIX E: DERIVATION OF FOUR NON-MARKOVIAN CORRECTION TERMS TO TRACE FUNCTION

When expanding the nonlinear action in Eq. (C11) to all orders in γ and to $\mathcal{O}(g^2)$, the nonvanishing contribution of joint perturbative order $\gamma^n g^2$ is obtained by inserting the (Fourier-transformed) g^2 decoration



$$= \iint d^d \tilde{\omega}_1 \cdots d^d \tilde{\omega}_4 dy_1 \cdots dy_4 \tilde{\varphi}(y_1, \tilde{\omega}_1) \partial_{y_2} \varphi(y_2, \tilde{\omega}_2) C_2(\tilde{\omega}_3 + \tilde{\omega}_4) \tilde{\varphi}(y_3, \tilde{\omega}_3) \partial_{y_4} \varphi(y_4, \tilde{\omega}_4) \times \delta(\tilde{\omega}_1 + \tilde{\omega}_2 + \tilde{\omega}_3 + \tilde{\omega}_4) \quad (E1)$$

into the expansion of the trace function $\langle \psi \tilde{\varphi} \rangle$ as


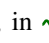


$$\begin{aligned} \mathcal{Q}(x_0, x, \omega) \delta(\omega + \omega') &= \sum_{n=0}^{\infty} \gamma^{2+n} \int d\omega_1 \cdots d\omega_n d\tilde{\omega}_1 \cdots d\tilde{\omega}_4 dz_1 \cdots dz_n dy_1 \cdots dy_4 \\ &\times \langle \psi(x, \omega) (-\lambda \tilde{\psi}(z_1, \omega_1) \varphi(z_1, \omega_1) \psi(z_1, \omega_1)) (-\kappa \tilde{\varphi}(z_2, \omega_2) \tilde{\psi}(z_2, \omega_2) \varphi(z_2, \omega_2) \psi(z_2, \omega_2)) \cdots \\ &(-\kappa \tilde{\varphi}(z_{n-1}, \omega_{n-1}) \tilde{\psi}(z_{n-1}, \omega_{n-1}) \varphi(z_{n-1}, \omega_{n-1}) \psi(z_{n-1}, \omega_{n-1})) (\sigma \tilde{\varphi}(z_n, \omega_n) \tilde{\psi}(z_n, \omega_n) \varphi(z_n, \omega_n)) \\ &\times \varphi(x_0, \omega') g^2 \tilde{\varphi}(y_1, \tilde{\omega}_1) \partial_{y_2} \varphi(y_2, \tilde{\omega}_2) C_2(\tilde{\omega}_3 + \tilde{\omega}_4) \tilde{\varphi}(y_3, \tilde{\omega}_3) \partial_{y_4} \varphi(y_4, \tilde{\omega}_4) \times \delta(\tilde{\omega}_1 + \tilde{\omega}_2 + \tilde{\omega}_3 + \tilde{\omega}_4) \rangle. \end{aligned} \quad (E2)$$

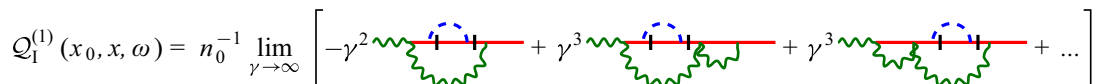
As usual, we employ Wick’s theorem to evaluate this average over Gaussian random variables: When expanding the average $n_0^{-1} \langle \psi(x, \omega) \tilde{\varphi}(x_0, \omega') \rangle$ in powers of γ and g , as shown in Eq. (E2), the resulting coefficients are averages over finite products of $\varphi_1 \cdots \varphi_{j_1}, \tilde{\varphi}_1 \cdots \varphi_{j_2}, \psi_1 \cdots \psi_{j_3}$, and $\tilde{\psi}_1 \cdots \tilde{\psi}_{j_4}$ fields [where $\varphi_i = \varphi(z_i, \omega_i)$, etc.] with respect to the Gaussian measure [defined by the action in Eq. (11) for $\gamma = 0$]. Each of those coefficients is evaluated using Wick’s theorem, i.e.,

$$\langle \psi_1 \cdots \psi_{j_1} \tilde{\psi}_1 \cdots \tilde{\psi}_{j_2} \varphi_1 \cdots \varphi_{j_3} \tilde{\varphi}_1 \cdots \tilde{\varphi}_{j_4} \rangle_{S; \gamma=0} = \sum_{\text{pairings}} \prod_{(k_m, \ell_m)} \langle \phi_{k_m} \phi_{\ell_m} \rangle_{S; \gamma=0}, \quad (E3)$$

where the sum runs over all possible pairwise pairings of the $j_1 + j_2 + j_3 + j_4$ indices, and we use ϕ in lieu of $\varphi, \tilde{\varphi}, \psi, \tilde{\psi}$ to alleviate notation. Although the number of possible combinations of such pairings is very large, the right-hand side of Eq. (E3) drastically simplifies because most of the pairwise averages vanish under the Gaussian average. Again, as in the case of $g = 0$ (cf. Appendix B), the only nonvanishing Gaussian correlators are those of the form $\langle \varphi \tilde{\varphi} \rangle, \langle \psi \tilde{\psi} \rangle$ as given by Eqs. (D3) and (D4). Thus, the sum over averages in Eq. (E2) simplifies into a sum over integrals over products of these two Gaussian propagators. The integrals run over n internal spatial variables z_1, \dots, z_n which stem from the expansion in γ^n , and four internal spatial variables y_1, \dots, y_4 which stem from the expansion in g^2 (and thus are related to the non-Markovian correction). Analogously, the integration also runs over n frequencies $\omega_1, \dots, \omega_n$ stemming from the γ^n expansion and four frequencies $\tilde{\omega}_1, \dots, \tilde{\omega}_4$ from the g^2 expansion. The integral over the internal space variables z_1, \dots, z_n simplifies significantly, since the corresponding $\langle \psi \tilde{\psi} \rangle$ propagators [cf. Eq. (D4)] are proportional to spatial δ functions. This results in all internal space coordinates to identify as $z_1 = \dots = z_n = x$.

The integral over the internal spatial coordinates y_1, \dots, y_4 appearing in the four φ and $\tilde{\varphi}$ fields in Eq. (E2), however, is less trivial as it involves the correlators (“propagators”) of $\langle \varphi \tilde{\varphi} \rangle$. Likewise, the integration over $\tilde{\omega}_1, \dots, \tilde{\omega}_4$, further involves the correlator of the driving noise, $C_2(\tilde{\omega}_3 + \tilde{\omega}_4)$. Hence, the integrals stemming from the g^2 expansion need to be dealt with more carefully: The four fields $\tilde{\varphi}(y_1, \tilde{\omega}_1) \partial_{y_2} \varphi(y_2, \tilde{\omega}_2) \tilde{\varphi}(y_3, \tilde{\omega}_3) \partial_{y_4} \varphi(y_4, \tilde{\omega}_4)$ appearing in every term of Eq. (E2) have to be paired up [according to Eq. (E3)] with another creation field $\tilde{\varphi}(z_i)$ or annihilation field $\tilde{\varphi}(z_i)$ appearing in Eq. (E2), respectively, in order to have a nonvanishing contribution [cf. Eq. (D3)]. Up to permutation of indices, each of these possible combinations [which we refer to as “Wick pairings,” Eq. (E3)] can fundamentally be grouped into four different ways that are best understood diagrammatically: In any case, each of the two $\varphi(y_i) \partial_{y_j} \tilde{\varphi}(y_j)$ attaches via Wick pairing to a $\varphi(z_k) \tilde{\varphi}(z_\ell)$ field appearing in the terms of Eq. (E2). Concurrently, $\tilde{\varphi}(z_k), \varphi(z_\ell)$ Wick-pair with two other corresponding fields, giving rise to connected $\langle \varphi \tilde{\varphi} \rangle$ —“propagators” and so on. Thereby, the Wick pairing of $\varphi(y_i) \partial_{y_j} \tilde{\varphi}(y_j)$, diagrammatically speaking, splits an existing propagator in the γ^n expansion into two or, as shown below, in three.

In the expansion to order γ^n , there is one propagator from x_0 to x (transition) and n propagators from x to x (return) represented by loop diagrams. The g vertex can thus occur in four different ways (Fig. 2), to be distinguished by whether and how the g vertex enters into the initial transition propagator, , in  +  + ..., Eq. (D1), or into any of the return propagators . First, we consider $\mathcal{Q}_1^{(1)}$ (diagram I in Fig. 2), the case of the correlation coupling appearing twice within the same return propagator leading to the diagrammatic sum



$$\mathcal{Q}_1^{(1)}(x_0, x, \omega) = n_0^{-1} \lim_{\gamma \rightarrow \infty} \left[-\gamma^2 \text{diagram} + \gamma^3 \text{diagram} + \gamma^3 \text{diagram} + \dots \right] \quad (E4)$$

$$= n_0^{-1} \lim_{\gamma \rightarrow \infty} \left[\gamma^2 \sum_{r=0}^{\infty} \left(\gamma \text{---} \right)^r \times \text{---} \times \sum_{s=0}^{\infty} \left(\gamma \text{---} \right)^s \times \text{---} \right] \tag{E5}$$

$$= -\frac{1}{-i\omega (R(x, \omega))^2} \iint dy_1 dy_2 d\tilde{\omega} (\partial_{y_1} T(x, y_1, \omega)) (\partial_{y_2} T(y_1, y_2, \omega - \tilde{\omega})) T(y_2, x, \omega) C_2(\tilde{\omega}). \tag{E6}$$

In the last line, we replaced the geometric sums in Eq. (E5) by the expression found for τ_R in Eq. (D17). To be precise, this is not a matter of trivially renormalizing τ to τ_R , as the sums appearing in Eq. (E5) are in fact renormalizations of λ and σ , respectively,

$$-\lambda_R = (-\lambda)\gamma \sum_{r=0}^{\infty} \left(\gamma \text{---} \right)^r = \gamma(-\lambda) + \gamma(-\lambda) \sum_{r=1}^{\infty} (-\gamma\kappa R(x, \omega))^r \xrightarrow{\gamma \rightarrow \infty} -\frac{1}{R(x, \omega)} \tag{E7}$$

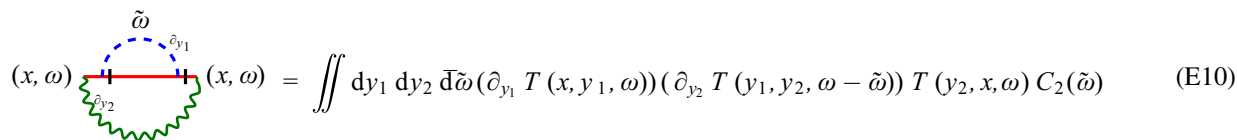
$$\sigma_R = \sigma\gamma \sum_{r=0}^{\infty} \left(\gamma \text{---} \right)^r = \gamma\sigma + \gamma\sigma \sum_{r=1}^{\infty} (-\gamma\kappa R(x, \omega))^r \xrightarrow{\gamma \rightarrow \infty} \frac{n_0}{R(x, \omega)}, \tag{E8}$$

where again we made use of the definition $n_0 = \sigma\kappa^{-1}$. However, comparing to Eq. (D17), they renormalize identically, as does κ ,

$$-\kappa_R = (-\kappa)\gamma \sum_{r=0}^{\infty} \left(\gamma \text{---} \right)^r = \gamma(-\kappa) \sum_{r=0}^{\infty} (-\gamma\kappa R(x, \omega))^r \xrightarrow{\gamma \rightarrow \infty} -\frac{1}{R(x, \omega)} \tag{E9}$$

to be used below.

Another identity entering into expressing $\mathcal{Q}_I^{(1)}$, Eq. (E4), as Eq. (E6), is the key ingredient of $\mathcal{Q}_I^{(1)}$:



$$(x, \omega) \text{---} \text{---} (x, \omega) = \iint dy_1 dy_2 d\tilde{\omega} (\partial_{y_1} T(x, y_1, \omega)) (\partial_{y_2} T(y_1, y_2, \omega - \tilde{\omega})) T(y_2, x, \omega) C_2(\tilde{\omega}) \tag{E10}$$

Considering $\mathcal{Q}_{II}^{(1)}$, shown as diagram II in Fig. 2, next, the two g vertices may be inserted into two different return propagators --- of a diagram in the expansion Eq. (D1),

$$\mathcal{Q}_{II}^{(1)}(x_0, x, \omega) = n_0^{-1} \lim_{\gamma \rightarrow \infty} \left[\gamma^3 \text{---} \text{---} \text{---} - \gamma^4 \text{---} \text{---} \text{---} - \gamma^4 \text{---} \text{---} \text{---} - \gamma^4 \text{---} \text{---} \text{---} + \dots \right] \tag{E11}$$

$$= n_0^{-1} \lim_{\gamma \rightarrow \infty} \left[\gamma^3 \sum_{r=0}^{\infty} \left(\gamma \text{---} \right)^r \times \text{---} \times \sum_{s=0}^{\infty} \left(\gamma \text{---} \right)^s \times \text{---} \times \sum_{t=0}^{\infty} \left(\gamma \text{---} \right)^t \times \text{---} \right] \tag{E12}$$

$$= n_0^{-1} \lim_{\gamma \rightarrow \infty} \left[\gamma^3 \frac{1}{-i\omega} \frac{-\lambda\gamma}{1 + \gamma\kappa R(x, \omega)} \times \text{---} \times \sum_{s=0}^{\infty} \left(\gamma \text{---} \right)^s \times \text{---} \times \frac{\sigma\gamma}{1 + \gamma\kappa R(x, \omega)} T(x_0, x, \omega) \right] \tag{E13}$$

Here, we made use again of the geometric sums in Eq. (D17) as well as Eqs. (E7)–(E9), which features three times in Eq. (E11), once with dummy index r , once with s , and once with t . The central one, running with index s , differs from the others by the (blue) dashed line that represents the noise carrying momentum $\tilde{\omega}$ thus bypassing the loops, so that only $\omega - \tilde{\omega}$ flows through loops summed over. Using Eq. (E9) in this loop, the effective vertex of $\mathcal{Q}_{II}^{(1)}(x_0, x, \omega)$ is





$$(x, \omega) \text{---} \text{---} (x, \omega) \times \sum_{s=0}^{\infty} \left(\gamma \text{---} \right)^s \times \text{---} \tag{E14}$$

$$= \iint dy_1 dy_2 d\tilde{\omega} (\partial_{y_1} T(x, y_1, \omega)) T(y_1, x, \omega - \tilde{\omega}) \frac{1}{R(x, \omega - \tilde{\omega})} (\partial_{y_2} T(x, y_2, \omega - \tilde{\omega})) T(y_2, x, \omega) C_2(\tilde{\omega}), \tag{E15}$$

to be contrasted with Eq. (E10), the effective vertex of $\mathcal{Q}_I^{(1)}(x_0, x, \omega)$.

Inserting the result (E15) into Eq. (E13), and using $n_0 = \sigma/\kappa$, we obtain an explicit formula

$$\mathcal{Q}_{II}^{(1)}(x_0, x, \omega) = \frac{1}{-i\omega} \frac{T(x_0, x)}{(R(x, \omega))^2} \iint dy_1 dy_2 d\tilde{\omega} \frac{(\partial_{y_1} T(x, y_1, \omega))T(y_1, x, \omega - \tilde{\omega})}{R(x, \omega - \tilde{\omega})} (\partial_{y_2} T(x, y_2, \omega - \tilde{\omega}))T(y_2, x, \omega)C_2(\tilde{\omega}). \tag{E16}$$

Third, we consider $\mathcal{Q}_{III}^{(1)}$, shown as diagram III in Fig. 2, the case of the transition propagator, , coupling to one of the return propagators, , via $C_2(\omega)$ which results in the diagrammatic expansion

$$\mathcal{Q}_{III}^{(1)}(x_0, x, \omega) = n_0^{-1} \lim_{\gamma \rightarrow \infty} \left[-\gamma^2 \text{diagram} + \gamma^3 \text{diagram} + \gamma^3 \text{diagram} + \dots \right] \tag{E17}$$

$$= n_0^{-1} \lim_{\gamma \rightarrow \infty} \left[\gamma^3 \sum_{r=0}^{\infty} \left(\gamma \text{diagram} \right)^r \times \text{diagram} \times \sum_{s=0}^{\infty} \left(\gamma \text{diagram} \right)^s \times \text{diagram} \right] \tag{E18}$$

$$= n_0^{-1} \lim_{\gamma \rightarrow \infty} \left[\gamma^3 \frac{1}{-i\omega} \frac{(-\lambda)\gamma}{1 + \gamma\kappa R(x, \omega)} \times \text{diagram} \times \sum_{s=0}^{\infty} \left(\gamma \text{diagram} \right)^s \times \text{diagram} \right] \tag{E19}$$

where we made use of the renormalization of λ , Eq. (E7). For the remaining diagram in Eq. (E19), which differs from Eq. (E15) only by an incoming transition propagator instead of a return propagator, we find

$$\begin{aligned} \text{diagram} \times \sum_{s=0}^{\infty} \left(\gamma \text{diagram} \right)^s \times \text{diagram} &= \iint dy_1 dy_2 d\tilde{\omega} (\partial_{y_1} T(x_0, y_1, \omega))T(y_1, x, \omega - \tilde{\omega}) \\ &\times \frac{\gamma^{(-\kappa)}}{1 + \gamma\kappa R(x, \omega - \tilde{\omega})} (\partial_{y_2} T(x, y_2, \omega - \tilde{\omega}))T(y_2, x, \omega)C_2(\tilde{\omega}). \end{aligned} \tag{E20}$$

Inserting the result of Eq. (E20) into Eq. (E19), one obtains

$$\mathcal{Q}_{III}^{(1)}(x_0, x, \omega) = -\frac{1}{-i\omega} \frac{1}{R(x, \omega)} \iint dy_1 dy_2 d\tilde{\omega} \frac{(\partial_{y_1} T(x_0, y_1, \omega))T(y_1, x, \omega - \tilde{\omega})}{R(x, \omega - \tilde{\omega})} (\partial_{y_2} T(x, y_2, \omega - \tilde{\omega}))T(y_2, x, \omega)C_2(\tilde{\omega}). \tag{E21}$$

Finally, we consider $\mathcal{Q}_{IV}^{(1)}$, shown as diagram IV in Fig. 2, where two g vertices couple into the incoming transition propagator,

$$\mathcal{Q}_{IV}^{(1)}(x_0, x, \omega) = n_0^{-1} \lim_{\gamma \rightarrow \infty} \left[\gamma \text{diagram} - \gamma^2 \text{diagram} + \gamma^3 \text{diagram} + \dots \right] \tag{E22}$$

$$= n_0^{-1} \lim_{\gamma \rightarrow \infty} \left[\gamma \sum_{r=0}^{\infty} \left(\gamma \text{diagram} \right)^r \text{diagram} \right] \tag{E23}$$

$$= n_0^{-1} \lim_{\gamma \rightarrow \infty} \left[\gamma \frac{1}{-i\omega} \frac{(-\lambda)\gamma}{1 + \gamma\kappa R(x, \omega)} \iint dy_1 dy_2 d\tilde{\omega} (\partial_{y_1} T(x_0, y_1, \omega))(\partial_{y_2} T(y_1, y_2, \omega - \tilde{\omega}))T(y_2, x, \omega)C_2(\tilde{\omega}) \right] \tag{E24}$$

$$= \frac{1}{-i\omega} \frac{1}{R(x, \omega)} \iint dy_1 dy_2 d\tilde{\omega} (\partial_{y_1} T(x_0, y_1, \omega))(\partial_{y_2} T(y_1, y_2, \omega - \tilde{\omega}))T(y_2, x, \omega)C_2(\tilde{\omega}). \tag{E25}$$

The trace function corrected to leading order in the external noise is thus given by

$$\mathcal{Q}(x_0, x, \omega) = \frac{T(x_0, x, \omega)}{(-i\omega)R(x, \omega)} + g^2 [\mathcal{Q}_I^{(1)} + \mathcal{Q}_{II}^{(1)} + \mathcal{Q}_{III}^{(1)} + \mathcal{Q}_{IV}^{(1)}] + \mathcal{O}(g^3). \tag{E26}$$

Comparing the four correction terms, $\mathcal{Q}_I^{(1)}, \dots, \mathcal{Q}_{IV}^{(1)}$, it turns out that they draw on two different integrals,

$$\mathcal{J}_1(x_0, x, \omega) = \iint dy_1 dy_2 d\tilde{\omega} (\partial_{y_1} T(x_0, y_1, \omega))(\partial_{y_2} T(y_1, y_2, \omega - \tilde{\omega}))T(y_2, x, \omega)C_2(\tilde{\omega}), \tag{E27}$$

$$\mathcal{J}_2(x_0, x, \omega) = \iint dy_1 dy_2 d\tilde{\omega} \frac{(\partial_{y_1} T(x_0, y_1, \omega))T(y_1, x, \omega - \tilde{\omega})}{R(x, \omega - \tilde{\omega})} (\partial_{y_2} T(x, y_2, \omega - \tilde{\omega}))T(y_2, x, \omega)C_2(\tilde{\omega}), \tag{E28}$$

with \mathcal{J}_1 entering into $\mathcal{Q}_I^{(1)}$ and $\mathcal{Q}_{IV}^{(1)}$, Eqs. (E6) and (E25), and \mathcal{J}_2 entering into $\mathcal{Q}_{II}^{(1)}$ and $\mathcal{Q}_{III}^{(1)}$, Eqs. (E16) and (E21),

$$\mathcal{Q}_I^{(1)}(x_0, x, \omega) = -\frac{1}{-i\omega} \frac{T(x_0, x, \omega)}{(R(x, \omega))^2} \mathcal{J}_1(x, x, \omega), \tag{E29}$$

$$\mathcal{Q}_{\text{II}}^{(1)}(x_0, x, \omega) = \frac{1}{-i\omega} \frac{T(x_0, x, \omega)}{(R(x, \omega))^2} \mathcal{J}_2(x, x, \omega), \quad (\text{E30})$$

$$\mathcal{Q}_{\text{III}}^{(1)}(x_0, x, \omega) = -\frac{1}{-i\omega} \frac{1}{R(x, \omega)} \mathcal{J}_2(x_0, x, \omega), \quad (\text{E31})$$

$$\mathcal{Q}_{\text{IV}}^{(1)}(x_0, x, \omega) = \frac{1}{-i\omega} \frac{1}{R(x, \omega)} \mathcal{J}_1(x_0, x, \omega). \quad (\text{E32})$$

Equation (E26) simplifies further when factorizing out the term to order g^0 :

$$\mathcal{Q}(x_0, x, \omega) = \frac{T(x_0, x, \omega)}{(-i\omega)R(x, \omega)} \left[1 + g^2 \left(\frac{\mathcal{J}_1(x_0, x, \omega) - \mathcal{J}_2(x_0, x, \omega)}{T(x_0, x, \omega)} - \frac{\mathcal{J}_1(x, x, \omega) - \mathcal{J}_2(x, x, \omega)}{R(x, \omega)} \right) \right] + \mathcal{O}(g^3). \quad (\text{E33})$$

To simplify notation, we introduce

$$T^{(2)}(x_0, x, \omega) = \mathcal{J}_1(x_0, x, \omega) - \mathcal{J}_2(x_0, x, \omega) \quad (\text{E34})$$

$$= \iint dy_1 dy_2 d\tilde{\omega} \left[(\partial_{y_2} T(y_1, y_2, \omega - \tilde{\omega})) - \frac{T(y_1, x, \omega - \tilde{\omega})}{R(x, \omega - \tilde{\omega})} (\partial_{y_2} T(x, y_2, \omega - \tilde{\omega})) \right] \\ \times (\partial_{y_1} T(x_0, y_1, \omega)) T(y_2, x, \omega) C_2(\tilde{\omega}) \quad (\text{E35})$$

$$= \iint dy_1 dy_2 (\partial_{y_1} T(x_0, y_1, \omega)) (\partial_{y_2} T(y_2, x, \omega)) \\ \times \int d\tilde{\omega} \left[\frac{T(y_1, x, \omega - \tilde{\omega})}{R(x, \omega - \tilde{\omega})} T(x, y_2, \omega - \tilde{\omega}) - T(y_1, y_2, \omega - \tilde{\omega}) \right] C_2(\tilde{\omega}), \quad (\text{E36})$$

where the last equality follows by integration by parts and rearranging terms, arriving at Eq. (29). Using $T^{(2)}(x_0, x, \omega)$ in Eq. (E33) it may be written as

$$\mathcal{Q}(x_0, x, \omega) = \frac{T(x_0, x, \omega) + g^2 T^{(2)}(x_0, x, \omega)}{(-i\omega)(R(x, \omega) + g^2 T^{(2)}(x, x, \omega))} + \mathcal{O}(g^3). \quad (\text{E37})$$

In keeping with the notation of $T^{(2)}$ as the g^2 correction to the transition probability, we henceforth write $T^{(0)}$ for what used to be called T , the contribution at $g = 0$. Collecting these terms into the *renormalized* T , we write

$$T(x_0, x, \omega) = T^{(0)}(x_0, x, \omega) + g^2 T^{(2)}(x_0, x, \omega) + \mathcal{O}(g^3) \quad (\text{E38})$$

and along the same lines the return probability

$$R(x, \omega) = T(x, x, \omega) = R^{(0)}(x, \omega) + g^2 R^{(2)}(x, \omega) + \mathcal{O}(g^3) = T^{(0)}(x, x, \omega) + g^2 T^{(2)}(x, x, \omega) + \mathcal{O}(g^3), \quad (\text{E39})$$

so that

$$\mathcal{Q}(x_0, x, \omega) = \frac{T(x_0, x, \omega)}{(-i\omega)R(x, \omega)} + \mathcal{O}(g^3). \quad (\text{E40})$$

APPENDIX F: DERIVATION OF EFFECTIVE TRANSITION PROBABILITY FOR BROWNIAN MOTION DRIVEN BY SELF-CORRELATED NOISE

To compute $T^{(2)}(x, \omega)$ in Eq. (E36), we first express the Fourier-transformed correlation function $\hat{C}_2(\omega)$ in terms of the inverse Laplace transform $\bar{C}_2(\beta)$, using

$$\hat{C}_2(\omega) = \int_{-\infty}^{\infty} dt e^{i\omega t} C(|t|) = \int_{-\infty}^{\infty} dt e^{i\omega t} \int_0^{\infty} d\beta e^{-\beta|t|} \bar{C}_2(\beta) \quad (\text{F1})$$

$$= 2 \int_0^{\infty} d\beta \left(\int_0^{\infty} dt \cos(\omega t) e^{-\beta t} \right) \bar{C}_2(\beta) \quad (\text{F2})$$

$$= \int_0^{\infty} d\beta \frac{2\beta}{\omega^2 + \beta^2} \bar{C}_2(\beta), \quad (\text{F3})$$

which facilitates the calculation of the convolution over $\tilde{\omega}$ in the second line of Eq. (E36), in particular when we consider exponential correlations, Eq. (35), in which case $\bar{C}_2(\beta) \propto \delta(\beta - \beta^*)$. We first consider the convolution of C_2

with $T^{(0)}$,

$$\int d\omega T(y_1, y_2, \omega - \tilde{\omega})C_2(\omega) = \int_0^\infty d\beta \int d\omega T(y_1, y_2, \omega - \tilde{\omega}) \frac{2\beta\bar{C}_2(\beta)}{\tilde{\omega}^2 + \beta^2} \tag{F4}$$

$$= \int_0^\infty d\beta \bar{C}_2(\beta)T(y_1, y_2, \omega + i\beta), \tag{F5}$$

where we have used that $T(y_1, y_2, \omega)$ cannot have any poles in the upper half plane, because its inverse Fourier transform $T(y_1, y_2, \tau)$ must vanish for all $\tau < 0$. If there were any poles in the upper half plane, the auxiliary path that for $\tau < 0$ must pass through the upper half plane would enclose them, producing $T(y_1, y_2, \tau) \neq 0$.

Considering, second, the convolution of C_2 with the term of the form $T^{(0)}T^{(0)}/R^{(0)}$ in Eq. (E36), we similarly obtain

$$\int d\tilde{\omega} \frac{T(y_1, x, \omega - \tilde{\omega})}{R(x, \omega - \tilde{\omega})} T(x, y_2, \omega - \tilde{\omega})C_2(\tilde{\omega}) = \int d\tilde{\omega} \chi_{\text{FPT}}^{(0)}(y_1, x_1, \omega - \tilde{\omega})T(x_1, y_2, \omega - \tilde{\omega}) \int_0^\infty d\beta \frac{2\beta\bar{C}_2(\beta)}{\tilde{\omega}^2 + \beta^2} \tag{F6}$$

$$= \int_0^\infty d\beta \bar{C}_2(\beta)\chi_{\text{FPT}}^{(0)}(y_1, x_1, \omega + i\beta)T(x_1, y_2, \omega + i\beta) \tag{F7}$$

$$= \int_0^\infty d\beta \bar{C}_2(\beta) \frac{T(y_1, x, \omega + i\beta)}{R(x, \omega + i\beta)} T(x_1, y_2, \omega + i\beta), \tag{F8}$$

where we made use of the Markovian formula, Eqs. (B23) and (6), $\chi_{\text{FPT}}^{(0)}(\omega) = T(x_0, x; \omega)/R(x; \omega)$, which is, like $T(y_1, y_2, \omega)$ above, a Fourier transform of a probability density that vanishes for all $\tau < 0$ and thus has no poles in the upper half plane.

Having performed the convolutions over $\tilde{\omega}$, turning them into easier integrals over β , what remains are the two spatial integrals over y_1 and y_2 ,

$$T^{(2)}(x_0, x, \omega) = \int_0^\infty d\beta \bar{C}_2(\beta) \iint dy_1 dy_2 \left[\frac{T(y_1, x, \omega + i\beta)}{R(x, \omega + i\beta)} T(x, y_2, \omega + i\beta) - T(y_1, y_2, \omega + i\beta) \right] \times (\partial_{y_1} T(x_0, y_1, \omega))(\partial_{y_2} T(y_2, x, \omega)). \tag{F9}$$

We proceed by calculating $T^{(2)}(x_0, x, \omega)$ for the particular case of Brownian motion, which has transition propagator

$$T(x_0, x, \omega) = \int d\tilde{k} \frac{e^{ik(x-x_0)}}{-i\omega + D_x k^2} = \frac{e^{-|x-x_0|\sqrt{\frac{-i\omega}{D_x}}}}{\sqrt{-4i\omega D_x}}. \tag{F10}$$

Beginning with the simpler integrand in Eq. (F9), the first term we consider is

$$\mathcal{I}_1(x_0, x, \omega) = \int_0^\infty d\beta \bar{C}_2(\beta) \iint dy_1 dy_2 T(y_1, y_2, \omega + i\beta)(\partial_{y_1} T(x_0, y_1, \omega))(\partial_{y_2} T(y_2, x, \omega)) \tag{F11}$$

$$= \int_0^\infty d\beta \bar{C}_2(\beta) \iint dy_1 dy_2 \iint dk dp dq \frac{e^{ik(y_2-y_1)}}{-i\omega + D_x k^2 + \beta} \frac{(ip)e^{ip(y_1-x_0)}}{-i\omega + D_x p^2} \frac{(-iq)e^{iq(x-y_2)}}{-i\omega + D_x q^2}. \tag{F12}$$

Integration over both y_1 and y_2 results in two delta functions $\delta(k - p)$ and $\delta(p - q)$, respectively. Integrating over both $d\tilde{k}$ and $d\tilde{q}$ then results in

$$\mathcal{I}_1(x_0, x, \omega) = \int_0^\infty d\beta \bar{C}_2(\beta) \int d\tilde{p} \frac{p^2 e^{ip(x_1-x_0)}}{(-i\omega + D_x p^2)^2 (-i\omega + D_x p^2 + \beta)}, \tag{F13}$$

which using partial fractions can be expressed in terms of the Markovian transition densities (cf. Eq. (125) of Ref. [28]),

$$\mathcal{I}_1(x_0, x, \omega) = \int_0^\infty d\beta \bar{C}_2(\beta) \int d\tilde{p} \left(\frac{1}{\beta} \frac{p^2 e^{ip(x_1-x_0)}}{(-i\omega + D p^2)^2} - \frac{1}{\beta^2} \frac{p^2 e^{ip(x_1-x_0)}}{-i\omega + D p^2} + \frac{1}{\beta^2} \frac{p^2 e^{ip(x_1-x_0)}}{-i\omega + D p^2 + \beta} \right) \tag{F14}$$

$$= - \int_0^\infty d\beta \bar{C}_2(\beta) \beta^{-2} (\partial_{x_1}^2) [-i\partial_\omega \beta T(x_0, x_1, \omega) - T(x_0, x_1, \omega) + T(x_0, x_1, \omega + i\beta)]. \tag{F15}$$

Expressing $T(x_0, x, \omega)$ as a Fourier transform in t further leads to

$$\mathcal{I}_1(x_0, x, \omega) = - \int_0^\infty d\beta \bar{C}_2(\beta) \int dt e^{i\omega t} \beta^{-2} [\beta t - 1 + e^{-\beta t}] (\partial_{x_1}^2) T(x_0, x_1, t) \tag{F16}$$

$$= - \int_0^\infty d\beta \bar{C}_2(\beta) \int dt e^{i\omega t} t^2 Y(\beta t) (\partial_{x_1}^2) T(x_0, x, t), \tag{F17}$$

where we introduced the dimensionless scaling function

$$Y(z) = \frac{e^{-z} - 1 + z}{z^2} \tag{F18}$$

with $Y(z) \xrightarrow{z \rightarrow 0} 1/2$ and $Y(z) \xrightarrow{z \gg 1} z^{-1}$. While $Y(z)$ is specific to Brownian motion, other stochastic processes give rise to similar scaling functions as Eq. (97) of Ref. [28] indicates for the case of an Ornstein-Uhlenbeck process.

The second contribution of Eq. (F9) is

$$\mathcal{I}_2(x_0, x, \omega) \tag{F19}$$

$$= \int_0^\infty d\beta \bar{C}_2(\beta) \iint dy_1 dy_2 \frac{T(y_1, x, \omega + i\beta)}{R(x, \omega + i\beta)} T(x, y_2, \omega + i\beta) (\partial_{y_1} T(x_0, y_1, \omega)) (\partial_{y_2} T(y_2, x, \omega)) \tag{F20}$$

$$= \int_0^\infty d\beta \bar{C}_2(\beta) \sqrt{4D_x(\beta - i\omega)} \iint dy_1 dy_2 \iint dk_1 dk_2 dp dq \times \frac{e^{ik_1(x_1 - y_1)}}{-i\omega + D_x k_1^2 + \beta} \frac{e^{ik_2(y_2 - x_1)}}{-i\omega + D_x k_2^2 + \beta} \frac{(ip)e^{ip(y_1 - x_0)}}{-i\omega + D_x p^2} \frac{(-iq)e^{iq(x - y_2)}}{-i\omega + D_x q^2}, \tag{F21}$$

using $1/R(x, \omega + i\beta) = 1/T(x, x, \omega + i\beta) = \sqrt{4D_x(\beta - i\omega)}$, Eq. (F10). Integrating over y_1 and y_2 produces two δ functions, $\delta(p - k_1)\delta(q - k_2)$. Using them when integrating over k_1, k_2 gives

$$\mathcal{I}_2(x_0, x, \omega) = \int_0^\infty d\beta \bar{C}_2(\beta) \sqrt{4D_x(\beta - i\omega)} \left(\int dq \frac{(-iq)}{(-i\omega + D_x q^2)(-i\omega + D_x q^2 + \beta)} \right) \times \left(\int dp \frac{(ip)e^{ip(x_1 - x_0)}}{(-i\omega + D_x p^2)(-i\omega + D_x p^2 + \beta)} \right). \tag{F22}$$

By symmetry, the integral over dq vanishes and thus $\mathcal{I}_2 = 0$. For Brownian motion, we thus obtain for $T^{(2)}(x_0, x, \omega)$, Eqs. (29) and (E36),

$$T^{(2)}(x_0, x, \omega) = -\mathcal{I}_1(x_0, x, \omega) = \int_0^\infty d\beta \bar{C}_2(\beta) \int dt e^{i\omega t} t^2 Y(\beta t) (\partial_{x_1}^2) T(x_0, x, t). \tag{F23}$$

By inverting the Fourier transform we further obtain

$$T^{(2)}(x_0, x, t) = \int_0^\infty d\beta \bar{C}_2(\beta) t^2 Y(\beta t) (\partial_{x_1}^2) T(x_0, x, t) \tag{F24}$$

$$= \Upsilon(t) (\partial_{x_1}^2) T(x_0, x_1, t), \tag{F25}$$

where we introduced the time-stretch function, Eq. (31),

$$\Upsilon(t) = \int_0^\infty d\beta \bar{C}_2(\beta) t^2 Y(\beta t) \tag{F26}$$

$$= \int_0^\infty d\beta \frac{\bar{C}_2(\beta)}{\beta^2} [e^{-\beta t} - 1 + \beta t]. \tag{F27}$$

Making use of the properties of the Laplace transform, we find

$$\int_0^\infty d\beta \beta^{-2} e^{-\beta t} \bar{C}_2(\beta) = \int_0^\infty ds s C_2(t + s), \tag{F28}$$

$$\int_0^\infty d\beta \beta^{-2} \bar{C}_2(\beta) = \int_0^\infty ds s C_2(s), \tag{F29}$$

$$\int_0^\infty d\beta \beta^{-1} t \bar{C}_2(\beta) = \int_0^\infty ds t C_2(s), \tag{F30}$$

and after some simple transformations,

$$\Upsilon(t) = \int_0^\infty ds (s C_2(t + s) - s C_2(s) + t C_2(s)) = \int_0^t ds (t - s) C_2(s) = \int_0^t ds \int_0^s du C_2(u), \tag{F31}$$

as in Eq. (31).

APPENDIX G: LIST OF EXPLICIT RESULTS FOR VISIT PROBABILITIES

The concrete perturbative corrections resulting from formulas (28) and (29) are often cumbersome expressions. The correction for the active thermal Brownian motion on a real line, characterized by Eq. (30), and with an exponentially correlated driving

noise is given implicitly via Eq. (34). This integral can be performed using *Mathematica* [62] and delivers

$$Q(x, \omega) = \frac{e^{-\sqrt{\frac{-i\omega x^2}{D_x}}}}{-i\omega} \left[1 + \frac{g^2 D_y}{D_x^2 \beta} \left(D_x \sqrt{(-i\omega)(\beta - i\omega)} \left(e^{-\frac{\sqrt{\beta - i\omega} \sqrt{-i\omega} |x|}} - 1 \right) + \frac{1}{2} \beta \sqrt{-iD_x \omega |x|} \right) \right]. \tag{G1}$$

In the joint limit of $\beta \rightarrow 0$ and $D_y \beta = w^2$ fixed, the moment-generating function becomes

$$Q(x, \omega) = \frac{e^{-\sqrt{\frac{-i\omega x^2}{D_x}}}}{-i\omega} \left[1 + \frac{g^2 w^2}{8 D_x^2} \left(x^2 - \sqrt{\frac{D_x x^2}{-i\omega}} \right) \right]. \tag{G2}$$

This corresponds to the visit probability of a Brownian motion with a random but fixed additional drift term y which is Gaussian distributed with mean zero and variance w^2 .

In Ref. [28], we developed a perturbative framework which was able to compute the moment-generating functions of first-passage-time distributions for processes of the form (21). This framework did not use field theory, but instead a functional perturbation theory. Since $Q(x, \omega) = \frac{1}{-i\omega} \chi_{\text{FPT}}(x, \omega)$, we here report the findings for two other models first reported there, for future reference.

First, we report the visit probability of an active Brownian motion on a ring of radius r , hence

$$\dot{x}_t = \xi_t + g y_t, \quad x_t \equiv x_t + 2\pi r. \tag{G3}$$

We then study the visit probability over a certain angle $\theta = \frac{x_1 - x_0}{r}$. As a shorthand, we further introduce the inverse diffusive timescale $\alpha^{-1} = r^2/D_x$. To leading perturbative order, the visit probability is then given by (see Eq. (127) of Ref. [28])

$$Q(\theta, \omega) = \frac{\cosh((\theta - \pi)\sqrt{-i\alpha^{-1}\omega})}{(-i\omega) \cosh(\pi\sqrt{-i\alpha^{-1}\omega})} + \frac{D_y g^2}{2D_x} \frac{\sqrt{-i\alpha^{-1}\omega} \tanh(\pi\sqrt{-i\alpha^{-1}\omega})}{-i\alpha^{-1}\beta\omega} \left[\frac{\cosh((\theta - \pi)\sqrt{\alpha^{-1}(\beta - i\omega)})}{\sinh(\pi\sqrt{\alpha^{-1}(\beta - i\omega)})} 2\sqrt{\alpha^{-1}(\beta - i\omega)} \right. \\ \left. + \frac{\cosh((\theta - \pi)\sqrt{-i\alpha^{-1}\omega})}{\cosh(\pi\sqrt{-i\alpha^{-1}\omega})} (\pi\bar{\beta} - 2\sqrt{\alpha^{-1}(\beta - i\omega)} \coth(\pi\sqrt{\alpha^{-1}(\beta - i\omega)})) + \frac{\sinh((\theta - \pi)\sqrt{-i\alpha^{-1}\omega})}{\sinh(\pi\sqrt{-i\alpha^{-1}\omega})} \bar{\beta}(\pi - \theta) \right]. \tag{G4}$$

In the limit of infinite radius, $r \rightarrow \infty$, one finds $\theta\sqrt{-i\alpha^{-1}\omega} \rightarrow \sqrt{-i\frac{\omega(x_1 - x_0)^2}{D_x}}$, and accordingly the Markovian result converges, as expected, to

$$\lim_{r \rightarrow \infty} \frac{\cosh((\theta - \pi)\sqrt{-i\alpha^{-1}\omega})}{(-i\omega) \cosh(\pi\sqrt{-i\alpha^{-1}\omega})} = \lim_{r \rightarrow \infty} \frac{1}{(-i\omega)} \frac{\cosh\left(\sqrt{-i\frac{\omega}{D_x}}|x_1 - x_0| - \sqrt{-i\frac{\omega}{D_x}}\pi r\right)}{\cosh\left(\sqrt{-i\frac{\omega}{D_x}}\pi r\right)} = \frac{e^{\sqrt{-i\frac{\omega}{D_x}}|x_1 - x_0|}}{-i\omega}. \tag{G5}$$

Analogously, a more involved computation using, for instance, *Mathematica* confirms that

$$\lim_{r \rightarrow \infty} Q^{\text{ring}}\left(\frac{x_1 - x_0}{r}, \omega\right) = Q^{\text{line}}(x_1 - x_0, \omega) \tag{G6}$$

with $Q^{\text{ring}}(\frac{x_1 - x_0}{r}, \omega)$ being the result in Eq. (G4) and $Q^{\text{line}}(x_1 - x_0, \omega)$ the perturbative result found in Eq. (G1).

Finally we consider the case of a harmonic trap, i.e.,

$$\dot{x}_t = -\alpha x + \xi_t + g y_t, \tag{G7}$$

which we refer to as an active thermal Ornstein-Uhlenbeck (ATO) process. The result is more compactly given in dimensionless units:

$$\bar{\beta} = \alpha^{-1}\beta, \quad \bar{x}_0 = x_0/\ell, \quad \bar{x}_1 = x_1/\ell, \quad \text{with } \ell = \sqrt{D_x \alpha^{-1}}. \tag{G8}$$

The Fourier-transformed visit probability is given in terms of parabolic cylinder functions $D_{-\nu}(x)$ [63] and reads (for $x_0 < x_1$) (see Eq. (100) or Ref. [28])

$$Q(x, \omega) = e^{\frac{\bar{x}_0^2 - \bar{x}_1^2}{4}} \frac{D_{i\alpha^{-1}\omega}(\bar{x}_0)}{(-i\omega) D_{i\alpha^{-1}\omega}(\bar{x}_1)} + \frac{g^2 D_y \bar{\beta}}{D_x (-i\omega) 2(\bar{\beta}^2 - 1) D_{i\alpha^{-1}\omega}(-\bar{x}_1)^2 D_{-\bar{\beta} + i\alpha^{-1}\omega}(-\bar{x}_1)} (-i\alpha^{-1}\omega) e^{\frac{\bar{x}_0^2 - \bar{x}_1^2}{4}} \\ \times [(\bar{\beta} + 1)(-i\alpha^{-1}\omega + 1) D_{-\bar{\beta} + i\alpha^{-1}\omega}(-\bar{x}_1) (D_{i\alpha^{-1}\omega}(-\bar{x}_0) D_{i\alpha^{-1}\omega - 2}(-\bar{x}_1) - D_{i\alpha^{-1}\omega - 2}(-\bar{x}_0) D_{i\alpha^{-1}\omega}(-\bar{x}_1)) \\ - 2(\bar{\beta} - i\alpha^{-1}\omega) D_{i\alpha^{-1}\omega - 1}(-\bar{x}_1) (D_{i\alpha^{-1}\omega}(-\bar{x}_0) D_{-\bar{\beta} + i\alpha^{-1}\omega - 1}(-\bar{x}_1) - D_{-\bar{\beta} + i\alpha^{-1}\omega - 1}(-\bar{x}_0) D_{i\alpha^{-1}\omega}(-\bar{x}_1))]. \tag{G9}$$

- [1] R. Zwanzig, Ensemble method in the theory of irreversibility, *J. Chem. Phys.* **33**, 1338 (1960).
- [2] F. Haake, Statistical treatment of open systems by generalized master equations, in *Quantum Statistics in Optics and Solid-State Physics* (Springer, Berlin, 1973), pp. 98–168.
- [3] R. Zwanzig, *Nonequilibrium Statistical Mechanics* (Oxford University Press, Oxford, UK, 2001).
- [4] S. N. Majumdar, Persistence in nonequilibrium systems, *Curr. Sci.* **77**, 370 (1999).
- [5] A. J. Bray, S. N. Majumdar, and G. Schehr, Persistence and first-passage properties in nonequilibrium systems, *Adv. Phys.* **62**, 225 (2013).
- [6] F. Aurzada and T. Simon, Persistence probabilities and exponents, in *Lévy Matters V*, Lecture Notes in Mathematics Vol. 2149 (Springer, Berlin, 2015), Chap. 3, pp. 183–224.
- [7] E. Schrödinger, Zur Theorie der Fall- und Steigversuche an Teilchen mit Brownscher Bewegung, *Z. Phys.* **16**, 289 (1915).
- [8] H. E. Daniels and F. Smithies, The probability distribution of the extent of a random chain, *Math. Proc. Cambridge Philos. Soc.* **37**, 244 (1941).
- [9] B. Gnedenko, Sur la distribution limite du terme maximum d'une série aléatoire, *Ann. Math.* **44**, 423 (1943).
- [10] D. A. Darling and A. J. F. Siebert, The first passage problem for a continuous Markov process, *Ann. Math. Stat.* **24**, 624 (1953).
- [11] E. J. Gumbel, *Statistics of Extremes* (Columbia University Press, New York, 1958).
- [12] R. Metzler, G. Oshanin, and S. Redner, *First-Passage Phenomena and Their Applications* (World Scientific, Singapore, 2014).
- [13] S. N. Majumdar, A. Pal, and G. Schehr, Extreme value statistics of correlated random variables: A pedagogical review, *Phys. Rep.* **840**, 1 (2020).
- [14] P. Hänggi and P. Jung, Colored noise in dynamical systems, in *Advances in Chemical Physics*, edited by I. Prigogine and S. A. Rice (Wiley, New York, 2007), pp. 239–326.
- [15] K. J. Wiese, S. N. Majumdar, and A. Rosso, Perturbation theory for fractional Brownian motion in presence of absorbing boundaries, *Phys. Rev. E* **83**, 061141 (2011).
- [16] P. Singh and A. Pal, Extremal statistics for stochastic resetting systems, *Phys. Rev. E* **103**, 052119 (2021).
- [17] S. N. Majumdar, A. J. Bray, S. J. Cornell, and C. Sire, Global Persistence Exponent for Nonequilibrium Critical Dynamics, *Phys. Rev. Lett.* **77**, 3704 (1996).
- [18] K. Oerding, S. J. Cornell, and A. J. Bray, Non-Markovian persistence and nonequilibrium critical dynamics, *Phys. Rev. E* **56**, R25 (1997).
- [19] M. Arutkin, B. Walter, and K. J. Wiese, Extreme events for fractional Brownian motion with drift: Theory and numerical validation, *Phys. Rev. E* **102**, 022102 (2020).
- [20] K. Malakar, V. Jemseena, A. Kundu, K. Vijay Kumar, S. Sabhapandit, S. N. Majumdar, S. Redner, and A. Dhar, Steady state, relaxation and first-passage properties of a run-and-tumble particle in one-dimension, *J. Stat. Mech.* (2018) 043215.
- [21] F. J. Sevilla, R. F. Rodríguez, and J. R. Gomez-Solano, Generalized Ornstein-Uhlenbeck model for active motion, *Phys. Rev. E* **100**, 032123 (2019).
- [22] L. Dabelow, S. Bo, and R. Eichhorn, Irreversibility in Active Matter Systems: Fluctuation Theorem and Mutual Information, *Phys. Rev. X* **9**, 021009 (2019).
- [23] A. Shee, A. Dhar, and D. Chaudhuri, Active Brownian particles: Mapping to equilibrium polymers and exact computation of moments, *Soft Matter* **16**, 4776 (2020).
- [24] D. Martin and T. A. de Pirey, AOUP in the presence of Brownian noise: A perturbative approach, *J. Stat. Mech.* (2021) 043205.
- [25] J. Łuczka, Non-Markovian stochastic processes: Colored noise, *Chaos* **15**, 026107 (2005).
- [26] L. Caprini and M. B. U. Marconi, Active particles under confinement and effective force generation among surfaces, *Soft Matter* **14**, 9044 (2018).
- [27] L. Caprini, U. M. B. Marconi, A. Puglisi, and A. Vulpiani, The entropy production of Ornstein-Uhlenbeck active particles: A path integral method for correlations, *J. Stat. Mech.* (2019) 053203.
- [28] B. Walter, G. Pruessner, and G. Salbreux, First passage time distribution of active thermal particles in potentials, *Phys. Rev. Res.* **3**, 013075 (2021).
- [29] A. J. F. Siebert, On the first passage time probability problem, *Phys. Rev.* **81**, 617 (1951).
- [30] M. Doi, Second quantization representation for classical many-particle system, *J. Phys. A: Math. Gen.* **9**, 1465 (1976).
- [31] L. Peliti, Path integral approach to birth-death processes on a lattice, *J. Phys. France* **46**, 1469 (1985).
- [32] P. C. Martin, E. D. Siggia, and H. A. Rose, Statistical dynamics of classical systems, *Phys. Rev. A* **8**, 423 (1973).
- [33] N. G. v. Kampen, *Stochastic Processes in Physics and Chemistry*, 3rd ed. (Elsevier, Amsterdam, 2007).
- [34] H. Risken, *The Fokker-Planck Equation* (Springer, Berlin, 1984).
- [35] G. Pruessner and R. Garcia-Millan, Field theories of active particle systems and their entropy production, [arXiv:2211.11906](https://arxiv.org/abs/2211.11906).
- [36] U. C. Täuber, M. Howard, and B. P. Vollmayr-Lee, Applications of field-theoretic renormalization group methods to reaction-diffusion problems, *J. Phys. A: Math. Gen.* **38**, R79 (2005).
- [37] J. Cardy, Reaction-diffusion processes, in *Non-equilibrium Statistical Mechanics and Turbulence*, edited by S. Nazarenko and O. V. Zaboronski, London Mathematical Society Lecture Note Series 355 (Cambridge University Press, Cambridge, UK, 2008), pp. 108–161, <http://www-thphys.physics.ox.ac.uk/people/JohnCardy/warwick.pdf>.
- [38] M. Kac, On distributions of certain Wiener functionals, *Trans. Am. Math. Soc.* **65**, 1 (1949).
- [39] K. Itô, Wiener integral and Feynman integral, in *Proceedings of the Fourth Berkeley Symposium on Mathematical Statistics and Probability*, Vol. 4 (University of California Press, Berkeley, USA, 1961), p. 227.
- [40] I. Bordeu, S. Amarteifio, R. Garcia-Millan, B. Walter, N. Wei, and G. Pruessner, Volume explored by a branching random walk on general graphs, *Sci. Rep.* **9**, 15590 (2019).
- [41] S. Nekovar and G. Pruessner, A field-theoretic approach to the wiener sausage, *J. Stat. Phys.* **163**, 604 (2016).
- [42] S. Amarteifio, Field theoretic formulation and empirical tracking of spatial processes, Ph.D. thesis, Imperial College London, 2019.
- [43] T. Guérin, M. Dolgushev, O. Bénichou, and R. Voituriez, Universal kinetics of imperfect reactions in confinement, *Commun. Chem.* **4**, 157 (2021).

- [44] J. Cardy, Field theory and nonequilibrium statistical mechanics (unpublished), lectures presented as part of the Troisieme Cycle de la Suisse Romande.
- [45] W. Horsthemke and R. Lefever, *Noise-Induced Transitions: Theory and Applications in Physics, Chemistry, and Biology*, 2nd ed. (Springer, Berlin, 2006).
- [46] P. Hänggi, The functional derivative and its use in the description of noisy dynamical systems, in *Stochastic Processes Applied to Physics*, edited by L. Pesquera and M. Rodriguez (World Scientific, Singapore, 1985), pp. 69–95.
- [47] N. van Kampen, Remarks on non-Markov processes, *Braz. J. Phys.* **28**, 90 (1998).
- [48] P. Langevin, Sur la théorie du mouvement brownien, *C. R. Acad. Sci.* **146**, 530 (1908).
- [49] C. W. Gardiner, *Handbook of Stochastic Methods: For Physics, Chemistry and the Natural Sciences*, 2nd ed. (Springer-Verlag, Berlin, 1997).
- [50] R. Kubo, The fluctuation-dissipation theorem, *Rep. Prog. Phys.* **29**, 255 (1966).
- [51] T. Sandev and Ž. Tomovski, *Fractional Equations and Models: Theory and Applications*, Developments in Mathematics Vol. 61 (Springer, Berlin, 2019).
- [52] M. Chaichian and A. Demichev, *Path Integrals in Physics: Volume I Stochastic Processes and Quantum Mechanics* (CRC Press, Boca Raton, FL, 2001).
- [53] R. P. Feynman and A. R. Hibbs, *Quantum Mechanics and Path Integrals*, Dover Books on Physics (Dover, Mineola, NY, 2010).
- [54] V. Popov, J. Niederle, and L. Hlavatý, *Functional Integrals in Quantum Field Theory and Statistical Physics*, Mathematical Physics and Applied Mathematics (Springer, Berlin, 2001).
- [55] I. Calvo and R. Sánchez, The path integral formulation of fractional Brownian motion for the general Hurst exponent, *J. Phys. A: Math. Theor.* **41**, 282002 (2008).
- [56] B. Meerson, O. Bénichou, and G. Oshanin, Path integrals for fractional Brownian motion and fractional Gaussian noise, [arXiv:2209.11722](https://arxiv.org/abs/2209.11722).
- [57] M. Le Bellac, *Quantum and Statistical Field Theory [Phenomenes critiques aux champs de jauge]*, translated by G. Barton (Oxford University Press, New York, 1991).
- [58] L. H. Ryder, *Quantum Field Theory*, 2nd ed. (Cambridge University Press, Cambridge, UK, 1996).
- [59] P. Jung and P. Hänggi, Dynamical systems: A unified colored-noise approximation, *Phys. Rev. A* **35**, 4464 (1987).
- [60] P. Hänggi, P. Talkner, and M. Borkovec, Reaction-rate theory: Fifty years after Kramers, *Rev. Mod. Phys.* **62**, 251 (1990).
- [61] U. C. Täuber, *Critical Dynamics* (Cambridge University Press, Cambridge, UK, 2014).
- [62] Wolfram Research, Inc., *Mathematica*, Version 12.3.1 (Champaign, IL, 2021).
- [63] I. S. Gradshteyn and I. Ryzhik, *Table of Integrals, Series, and Products*, 7th ed. (Academic Press, New York, 2007).